Contents

Part I

Development of the new land surface scheme SiBUC

Chapter 1

Basic concept of the SiBUC model

1.1 The energy budget at different surface condition

The radiative energy absorbed from the sun and the atmosphere is partitioned into fluxes of sensible, latent, and gound heat, and this partitioning (redistribution of absorbed energy) is strongly dependent on both the land cover characteristics and its hydrological state.

- When the surface is wet, as is common in irrigated agricultural areas and after rain events, the incoming radiation is mostly used for evapotranspiration. In that case, sensible heat flux and soil heat flux are usually much smaller than latent heat flux, and Bowen ratio is close to zero.

- On a bare dry land, the absorption of the incoming radiation results in a strong heating of the surface, which usually generates a strong turbulent sensible heat flux and large soil heat flux. In that case, there is no evaporation, and the Bowen ratio is infinite.

- When the surface is covered by a dense vegetation, water is extracted mostly from the plant root zone by transpiration. Thus, latent heat flux is dominant even if the soil surface is dry, but as long as there is enough water available in the root zone and plants are not under stress conditions.

- In the case of water body, as will be seen in **Chapter 3**, significant part of absorbed energy is not used in a diurnal cycle of energy budget, and handed over in a seasonal cycle. The diurnal variation of energy budget and surface temperature tend to be small. Therefore, the energy budget components of water body have seasonal lag compared to those of other surfaces.

- In the case of urban area, the surface is covered by inpermeable pavement which does not allow the evaporation of soil moisture. Then, strong heating of the surface occurs as is the case for bare soil. Due to the complex geometrical structure of urban canopy, as will be seen in **Chapter 2**, the characteristics of turbulent transfer process and the radiation absorption and exchange process are much different from other surfaces. Furthermore, artificial heat is released as an additional energy as a result of human activity. The urban thermal environment depends not only on the difference in physical properties such as reflectance and heat capacity but also on the geometrical structure. Owing to the multiple scattering effects within street canyon (between street and wall, between facing walls), the albedo of of urban area becomes smaller than flat surface (Aida, 1978). As street canyon becomes deeper, sky-view factor from wall and road becomes small, and propotion of long-wave radiative energy trapped inside the canyon becomes larger.

1.2 Heterogeneity of land surface and "mosaic" approach

At the grid resolution of atmospheric models, land-surfaces are very heterogeneous. This can be easily understood by looking at maps of soil, vegetation, topography, land-use patterns, etc. **Figure 1.1** shows a land-use map of Lake Biwa Basin, Japan. The domain of this area is 1 degree × 1 degree. Water surface and urbanized area are shown in white and blue color respectively.

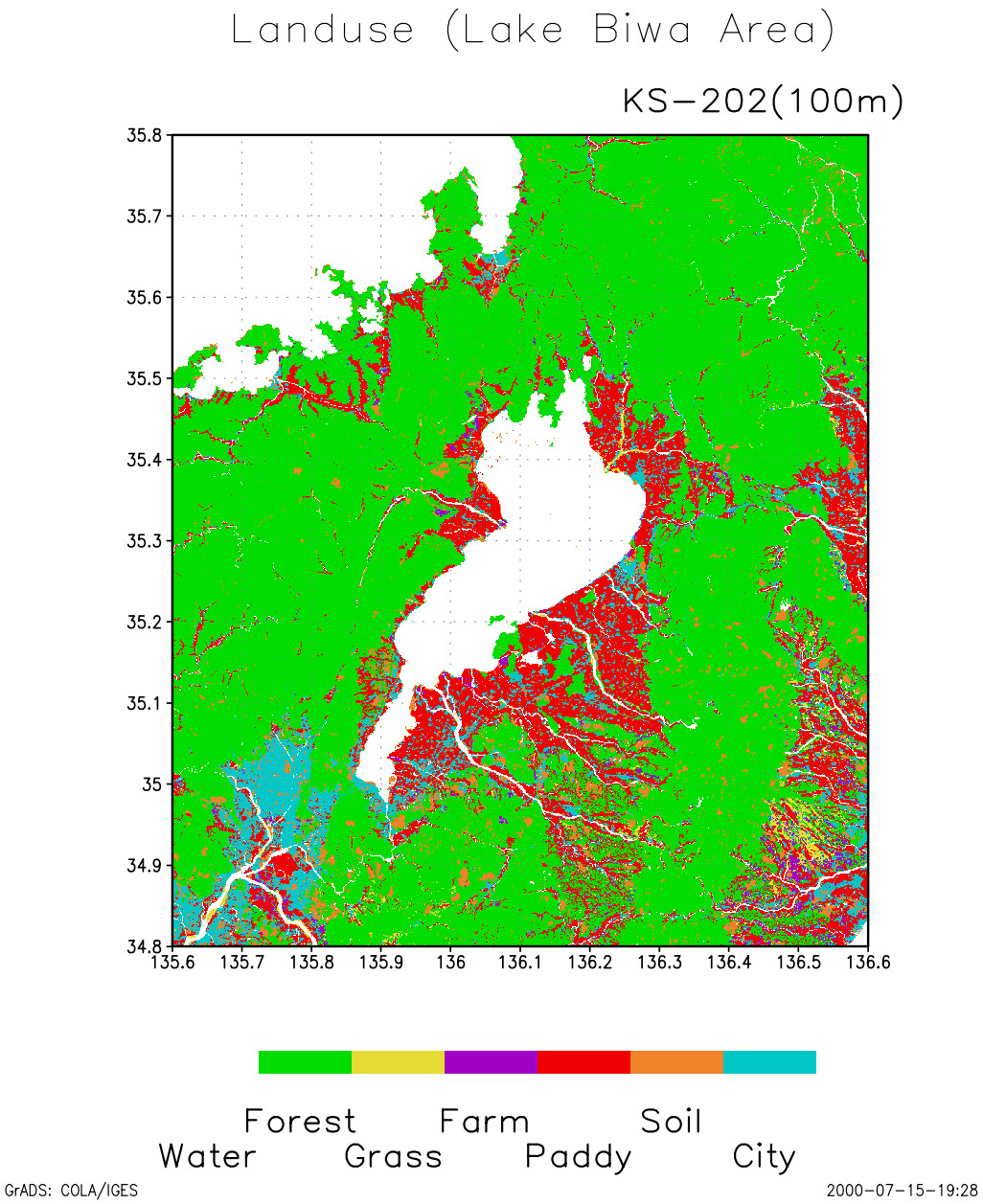

Figure 1.1: Land-use of Lake Biwa Basin (from KS-202)

In the numerical weather prediction model, the size of grid element is usually decided from the need of high accuracy and high computational efficiency. If the grid size is selected to eliminate the heterogeneity of land-surface, in another word, if the grid size is selected according to the 'minimum' size of land-use patch, it will become extremely small, and the number of grid elements will become enormous. Therefore, the problem of heterogeneity, off course, must be treated in

LSS (Land-Surface Scheme).
One solution is to find effective parameters to generate representative values of the whole grid square. A great deal of work has already been done on aggregation research (Michaud and Shuttleworth, 1997). Sometimes such a parameter aggregation is not possible because of high non-linearity between parameter and resulting fluxes.
Another way is to apply a "mosaic" type parameterization (Avissar and Pielke, 1989 ; Kimura, 1989). Such approach couples independently each land-use patch of the grid element to the atmosphere. The grid averaged surface fluxes are obtained by averaging the surface fluxes over each land-use weighted by its fractional area.

1.3 Surface elements and fractional area

The SiBUC (Simple Biosphere including Urban Canopy) model presented here uses "mosaic" approach to incorporate all kind of land-use into LSS. In the SiBUC model, the surface of each grid area is divided into three landuse categories and five components.

1. green area (vegetation canopy(c), ground(g))
2. urban area (urban canopy(uc), urban ground(ug))
3. water body (wb)

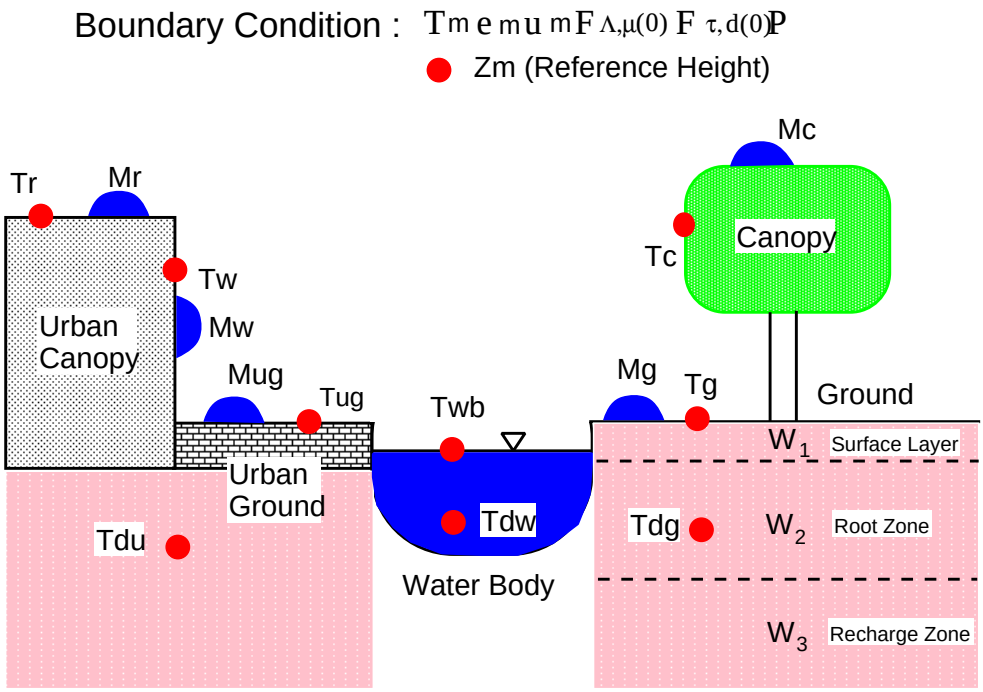

Figure 1.2: Schematic image of surface elements in SiBUC.

The schematic image of surface elements is shown in **Figure 1.2**. **1. green area** is a natural land surface area (forest, grassland, bare soil, etc.), and it is usually treated in most LSS. **2. urban area** is a artificial unpermeable surface (buildings, houses, pavement, etc.). **3. water body** is a inland water surface (ponds, rivers, lakes) or ocean surface.

Although the surface of real basin is a mixture of much more constituents, all surface elements must be classified into either of them. All the surface elements that are included in the same category are lumped and treated as "unit tile".
Each gridbox has specified fixed fractions of these three land-use (V_{ga}, V_{ua}, V_{wb}, respectively). Also canopy fractions within green area and urban area are also specified (V_c, V_{uc}, respectively).

$$V_{ga} + V_{ua} + V_{wb} = 1 \quad , \quad V_{ga} \geq 0, \quad V_{ua} \geq 0, \quad V_{wb} \geq 0 \tag{1.1}$$

$$0 \leq V_c \leq 1 \quad , \quad 0 \leq V_{uc} \leq 1 \tag{1.2}$$

Sensible heat, latent heat, and momentum fluxes are calculated separately by each sub-model (green area, urban canopy, water body). And the grid averaged surface fluxes are obtained by averaging the surface fluxes over each land-use weighted by its fractional area.

$$[F]_{total} = \sum_i [F]_i V_i = [F]_{ga} V_{ga} + [F]_{ua} V_{ua} + [F]_{wb} V_{wb} \tag{1.3}$$

- **green area**
  For the vegetation scheme, SiB (Sellers et al.,1986) is adopted. Some modification (simplification) from original SiB was done. The basic component of green area model will be described in **Chapter 4**. Now SiB2 (Sellers et al., 1994) can also be used as green area model (according to user's option).

- **urban area**
  A new urban canopy scheme which can account for complex structure of canyon geometry will be developed in **Chapter 2**. In the urban area, each roughness element is expressed by a square prism. All prisms are assumed to have the same width and to be evenly spaced, while they have their own roof heights. This description of urban canopy is used in the models for turbulent transfer. Radiation process is described precisely based on the "sky-view factor".

- **water body**
  Water body scheme is developed in **Chapter 3** based on force-restore model. Both diurnal and seasonal cycles of temperature are reproduced by this model.

The concept of "SiBUC" was firstly proposed by Tanaka et al.(1994). At that time, the definition of each fractional area are slightly differnt from current version. Also, sub-model for urban canopy was too simple in the original version. In this study, urban-canopy model is entirely replaced based on recent works.
The atmospheric boundary conditions (forcing variables) for SiBUC are the same as those for SiB and other land-surface schemes. And SiBUC has prognostic physical-state variables for each sub-model. Those are five surface temperatures, three deep layer temperatures, five interception water stores, and three soil moisture stores (see **Table 1.1**).
When the grid size is small (less than one kilometer), the arrangement and size of each land-use within grid area have small effects on heat fluxes, and only the fractional area must be considered to express the land-use heterogeneity. But when the grid size is large (more than ten kilometers), the land-use scale effects may appear, and the arrangement and size of each land-use should be considered too. This "scaling problem" will be discussed in **Part II**.
For the moment, SiBUC model just uses "mosaic" parameterization to calculate the grid average fluxes, and its application is limited to "basin-scale". SiBUC can be used for the understanding of basin-scale energy and water cycles. SiBUC will be used as a tool for investigating the scaling problem.

Table 1.1: Prognostic variables and boundary conditions for SiBUC

Prognostic Variables		
green area		
T_c	temperature for vegetation canopy	K
T_g	temperature for soil surface	K
T_d	temperature for deep soil in green area (daily mean of T_g)	K
M_c	interception water stored on canopy	m
M_g	interception water puddled on the ground	m
W_1	soil moisture wetness for surface layer	—
W_2	soil moisture wetness for root zone	—
W_3	soil moisture wetness for recharge layer	—
urban area		
T_r	temperature for building roof	K
T_w	temperature for building wall	K
T_{ug}	temperature for road	K
T_{du}	temperature for deep soil in urban area (daily mean of T_{ug})	K
M_r	interception water stored on building roof	m
M_w	interception water stored on building wall	m
M_{ug}	interception water puddled on the road	m
water body		
T_{wb}	temperature for water surface	K
T_{dw}	temperature for deep water (daily mean of T_{wb})	K
Boundary Conditions		
z_m	reference height	m
T_m	air temperature at z_m	K
e_m	vapor pressure at z_m	mb
u_m	wind speed at z_m	m s^{-1}
$S\downarrow$	downward short-wave radiation	W m^{-2}
$L\downarrow$	downward long-wave radiation	W m^{-2}
P	precipitation rate	m s−1

Chapter 2

Urban Canopy model

In this chapter, urban canopy model to be used as sub-model of land-surface scheme in mesoscale atmospheric model is developed. Due to the complexity and diverity of urban area, the model is formulated to be as general as possible to represent any kind of city. Masson (2000) has also presented a physically-based urban canopy scheme based on canyon geometry. The model presented here is different in the treatment of canyon structure. The model allows the existence of building elements of different height. Radiation and turbulent transfer process in the urban area, where various depth of street canyons are mixed, is modelled and formulated numerically. Then, the effects of geometrical structure of city elements on energy and radiation environment in urban area are discussed.

2.1 Street canyon geometry (k-story building)

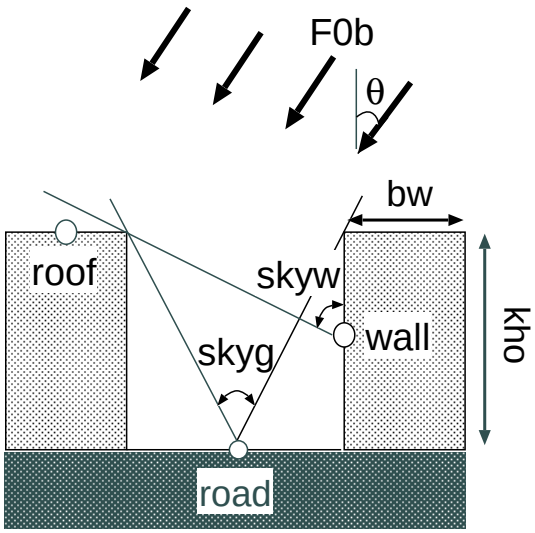

Figure 2.1: schematic image of street canyon, direct beam radiation, and sky-view factor

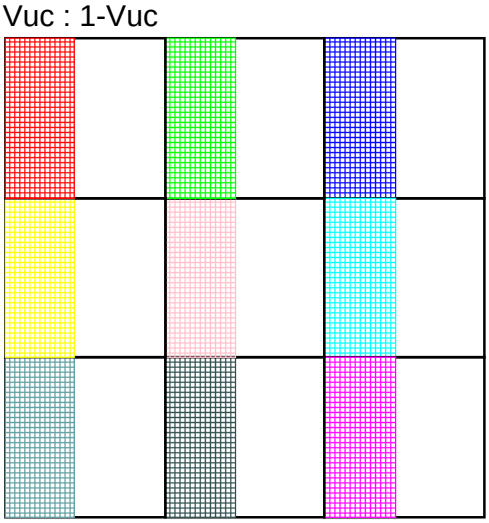

Figure 2.2: arrangement of street canyon (overlook from the sky)

The canyon concept, developed by urban climatologists (e.g., Oke(1987)), uses such a framework: it considers a single road, bordered by facing buildings. **Figure 2.1** shows the schematic image of street canyon, which is a basic component in the urban canopy model. In this figure, street canyon consists of building (width is b_w, height is kh_0 (k-story)) and road. If we consider the actual situation of city, road orientation (and also orientation of building wall) is mixed.

If we have detailed information about individual orientation and location of each buildings and roads, it may be possible to calculate energy and radiation budget for all individual elements. But in usual case, these information are difficult to obtain. Even though the street pattern is relatively regular, the directions of solar radiation and wind are changing in time. Then, we abandon to describe individual orientations of each street canyons.
In the calculation of radiation budget, it is assume that street is always perpendicular to the solar beam radiation (see **Figure 2.1**), and that buildings are located along identical roads, the length of which is considered far greater than their width (see **Figure 2.2**).

Table 2.1: Variables and parameters in urban canopy model

symbol	definition	unit
V_{ua}	fraction of urban area in a grid area	
V_{uc}	building coverage in V_{ua}	
n	highest number of building story	
k	number of building story in a canyon	
$r(k)$	fraction of k-story building	
h_0	unit height of story	m
b_w	building width	m
skyw, skyg	sky-view factor for wall and road	rad
C_d	drag coefficient	
$\alpha_i (i = r, w, ug)$	reflectance (albedo)	
$\varepsilon_i (i = r, w, ug)$	emissivity	
$c_i (i = r, w, ug)$	specific heat	J $m^{-3}K^{-1}$
$k_i (i = r, w, ug)$	thermal conductivity	$Wm^{-1}K^{-1}$
θ	incident angle of direct beam radiation	rad
$dS_i, uS_i (i = r, lw, rw, ug)$	downward and upward short-wave radiation	W m^{-2}
$dL_i, uL_i (i = r, w, ug)$	downward and upward long-wave radiation	W m^{-2}
$Rn_i (i = r, w, ug)$	net radiation	W m^{-2}
H_i (i=r,w,ug)	sensible heat flux from roof, wall, road	W m^{-2}
E_i (i=r,w,ug)	rates of evaporation from roof, wall, road	m s^{-1}
P_i (i=r,w,ug)	rate of rainfall interception by the roof,wall, road	m s^{-1}
D_i (i=r,w,ug)	rate of drainage from the roof, wall, road	m s^{-1}
$F_{0bi} (i = r, w, ug)$	direct beam component of short-wave radiation	W m^{-2}
$F_{0di} (i = r, w, ug)$	diffuse component of short-wave radiation	W m^{-2}
$F_{0ti} (i = r, w, ug)$	long-wave radiation (diffuse only)	W m^{-2}
P	rainfall rate	m s^{-1}
u_m	wind speed at reference height	K
T_m	temperature at reference height	K
e_m	vapor pressure at reference height	hPa
$T_i (i = r, w, ug, du, bi)$	temperature	K
$e_*(T_i)$ (i=r,w,ug)	saturation vapor pressure at T_i	hPa
M_i (i=r,w,ug)	water held on the roof, wall, road	m
S_i (i=r,w,ug)	maximum value of M_i	m
W_i (i=r,w,ug)	wetted fraction of roof, wall, road	
$r_i (i = r, w, du, au)$	aerodynamic resistance	s m^{-1}

where subscript $(-r, -w, -lw, -rw, -ug, -du, -bi)$ stands for roof, wall, left-side wall, right-side wall, road, soil, inside of building, respectively.

Basically, it is assumed that radiation energy is emitted from the center point of each component (roof, wall, road). And also "sky-view factor" is defined as the view angle from these center points. Using building coverage (or plan area density) (V_{uc}), the width of canyon air space is expressed as $b_w(1-V_{uc})/V_{uc}$. Therefore, sky-view factor for wall ($skyw$) and road ($skyg$) in a k-story canyon is expressed as follows.

$$\mathrm{skyw} = \arccos \frac{kh_0}{2\sqrt{\left(\frac{kh_0}{2}\right)^2 + \left(\frac{b_w(1-V_{uc})}{V_{uc}}\right)^2}} \tag{2.1}$$

$$\mathrm{skyg} = 2\arccos \frac{kh_0}{\sqrt{(kh_0)^2 + \left(\frac{b_w(1-V_{uc})}{2V_{uc}}\right)^2}} \tag{2.2}$$

Direct beam component of short-wave radiation (F_{0b}) incidents to the canyon with zenith angle θ, diffuse component of short-wave and long-wave radiation insident hemispherically.

2.2 Radiation transfer process

In this model, three components (roof, wall, road) are considered in the calculation of net radiation. Although there are various height of street canyon in the urban area, all canyons which have same height (k-story) are treated together. Assuming the situation of k-story canyon, radiation budget is calculated. Then, total net radiative energy for roof, wall, and road are calculated by integrating with roof height distribution function ($r(k)$). This is a basic concept of radiation process in urban canopy model.
Firstly, the partition of long-wave and short-wave radiation incident to each element is described.

2.2.1 partition of incident radiation

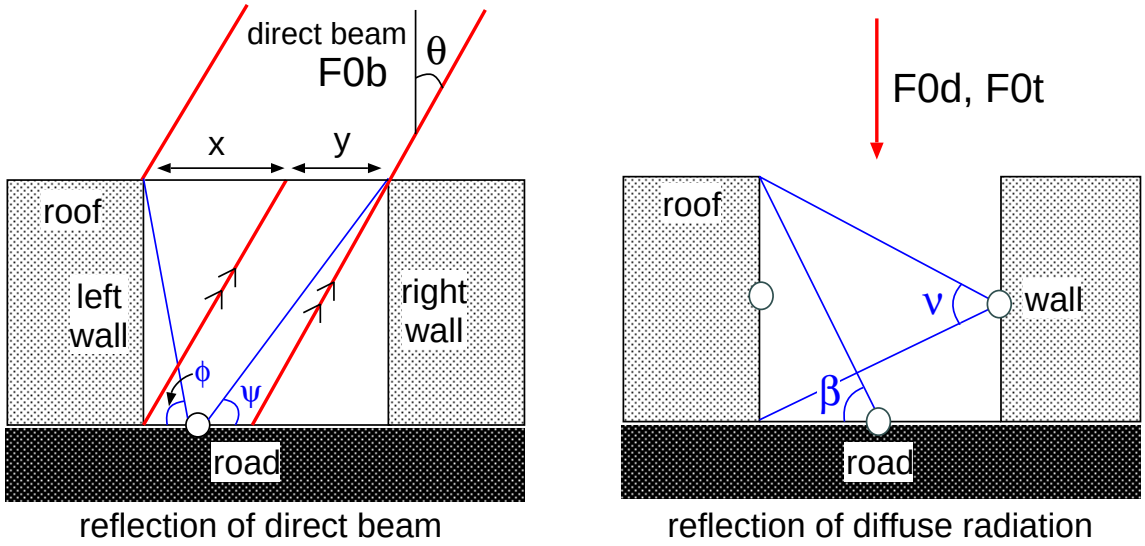

Figure 2.3: reflection to wall surface

Fraction of direct beam radiation incident to roof is same as building coverage (V_{uc}). As for wall and road, radiation is partitioned according to the incident zenith angle (θ). This partition is $x : y$ in **Figure 2.3**. where,

$$x : y = kh_0 \tan\theta : \frac{b_w(1 - V_{uc})}{V_{uc}} - kh_0 \tan\theta \tag{2.3}$$

Furthermore, radiation energy is partitioned according to the situation that the beam radiation incident to road or not.

$$\begin{aligned} \text{when} \quad \cos\theta &\geq \frac{kh_0}{\sqrt{(kh_0)^2 + \left(\dfrac{b_w(1 - V_{uc})}{V_{uc}}\right)^2}} \\ F_{0br} &= F_{0b} \times V_{uc} \quad F_{0bw} = F_{0b} V_{uc} \left(\frac{h_0}{b_w}\right) k \tan\theta \quad F_{0bg} = F_{0b}(1 - V_{uc}) - F_{0bw} \end{aligned} \tag{2.4}$$

$$\begin{aligned} \text{when} \quad \cos\theta &\leq \frac{kh_0}{\sqrt{(kh_0)^2 + \left(\dfrac{b_w(1 - V_{uc})}{V_{uc}}\right)^2}} \\ F_{0br} &= F_{0b} \times V_{uc} \quad F_{0bw} = F_{0b} \times (1 - V_{uc}) \quad F_{0bg} = 0 \end{aligned} \tag{2.5}$$

Although diffuse component of short-wave radiation and long-wave radiation incident to street canyon hemispherically, these radiations are partitioned according to the fraction viewed from high above the sky (see **Figure 2.2**). So no difuse radiation component is assigned to the wall.

$$F_{0dr} = F_{0d} \times V_{uc} \quad F_{0dw} = 0 \quad F_{0dg} = F_{0d}(1 - V_{uc}) \tag{2.6}$$

$$F_{0tr} = F_{0t} \times V_{uc} \quad F_{0tw} = 0 \quad F_{0tg} = F_{0t}(1 - V_{uc}) \tag{2.7}$$

2.2.2 Radiation budget at roof surface

In fact, roof may obtain some of radiation from neighboring buildings. But we don't use the detailed information about the arrangement of individual streets and buildings. Then, direct interaction of radiation between each street canyon is omitted in the model. For the roof surface, the formulation of radiation budget becomes very simple, because it is not necessary to consider the radiation which is reflected or emitted from other element.

$$dS_r = F_{0br} + F_{0dr} \qquad uS_r = \alpha_r(F_{0br} + F_{0dr}) \tag{2.8}$$

$$dL_r = F_{0tr} \qquad uL_r = \sigma\epsilon_r T_r^4 V_{uc} \tag{2.9}$$

$$Rn_r = dS_r + dL_r - uS_r - uL_r \tag{2.10}$$

2.2.3 Radiation budget at wall surface

In case of wall surface, the radiation scattered from facing wall and road are considered (single scatter only). In this model, the direction of street canyon is not considered, and it is described two dimensionally (see **Figure 2.1, 2.2**). And the wall which receive the direct beam is treated as "left" wall (right wall is shadow). In fact, the wall and street face to all directions. When the sun moves, some of wall which faces to the sun will receive the direct beam, and others not. This direct beam receiving wall is called as "left" wall.
The radiation incident to the left wall (dS_{lw}) consist of direct beam from sun and reflected radiation from road (reflection from right wall is omitted (double scatter)).

In the calculation of road reflection, view angle from the center point of direct beam receiving zone and diffuse radiation receiving zone are used (see **Figure 2.3**). These angles (ϕ and β in **Figure 2.3**) are expressed as follows.

$$\phi = \arctan \frac{2kh_0}{\frac{b_w(1-V_{uc})}{V_{uc}} - kh_0 \tan\theta}, \qquad \beta = \frac{\pi - \mathrm{skyg}}{2} \tag{2.11}$$

The radiation incident to the right wall (dS_{rw}) consist of reflected radiation from left wall and road. In the calculation of road and wall reflection, view angle from the center point of direct beam receiving zone and left wall are used (see **Figure 2.3**). These angles (ψ and ν in **Figure 2.3**) are expressed as follows.

$$\psi = \arctan \frac{2kh_0}{\frac{b_w(1-V_{uc})}{V_{uc}} + kh_0 \tan\theta}, \qquad \nu = \pi - 2\mathrm{skyw} \tag{2.12}$$

Reflection at wall and road is expressed by reflectance (α_w, α_g), and only single scattering is treated.

$$dS_{lw} = F_{0bw} + F_{0dw} + \alpha_w F_{0dw} \frac{\pi - 2\mathrm{skyw}}{\pi} + \alpha_g F_{0bg}(\frac{\phi}{\pi}) + \alpha_g F_{0dg} \frac{\pi - \mathrm{skyg}}{2\pi} \tag{2.13}$$

$$uS_{lw} = \alpha_w (F_{0bw} + F_{0dw}) \tag{2.14}$$

$$dS_{rw} = F_{0dw} + \alpha_w (F_{0bw} + F_{0dw}) \frac{\pi - 2\mathrm{skyw}}{\pi} + \alpha_g F_{0bg}(\frac{\psi}{\pi}) + \alpha_g F_{0dg} \frac{\pi - \mathrm{skyg}}{2\pi} \tag{2.15}$$

$$uS_{rw} = \alpha_w F_{odw} \tag{2.16}$$

Note that F_{0dw} in above equations are assumed to be zero.

left wall

1. direct beam ⇒ left wall
2. direct beam ⇒ road (ϕ) ⇒ left wall
3. diffuse ⇒ road (β) ⇒ left wall

right wall

1. direct beam ⇒ left wall (ν) ⇒ right wall
2. direct beam ⇒ road (ψ) ⇒ right wall
3. diffuse ⇒ road (β) ⇒ right wall

In case of wall, no long-wave radiation is received directly from the sky. Long-wave radiation emitted from road and facing wall are received according to the view angle (β and ν). In this case, left and right wall are treated in the same way. As for emission from wall, ratio of wall area to road area is multiplied.

$$dL_w = \sigma\epsilon_{ug} T_{ug}^4 \frac{\pi - \mathrm{skyg}}{2\pi}(1 - V_{uc}) + \sigma\epsilon_w T_w^4 \frac{\pi - 2\mathrm{skyw}}{\pi}(1 - V_{uc}) \frac{kh_0}{b_w \frac{(1-V_{uc})}{V_{uc}}} \tag{2.17}$$

$$uL_w = \sigma\varepsilon_w T_w^4 (1 - V_{uc}) \frac{kh_0}{b_w \frac{(1-V_{uc})}{V_{uc}}} \tag{2.18}$$

$$Rn_w = dS_{lw} + dS_{rw} + 2dL_w - uS_{lw} - uS_{rw} - 2uL_w \tag{2.19}$$

2.2.4 Radiation budget at road surface

There are two cases for direct beam radiation to incident to the road or not, depending on the solar angle. When there is no direct beam on the road, F_{0bg} in **eq.(2.20), (2.21)** becomes zero.

As for the fraction of reflected radiation from the wall, view angle is from the center point of the wall. Note that the direct beam does not incident to left wall, F_{0bw} in **eq. (2.20)** is only for left wall. Reflected short-wave radiation and emitted long-wave radiation are described in the same way as mentioned above.

$$
\begin{aligned}
dS_{ug} &= F_{0bg} + F_{0dg} + \alpha_w(F_{0bw} + 2F_{0dw})\frac{\text{skyw}}{\pi} && (2.20)\\
uS_{ug} &= \alpha_{ug}(F_{0bg} + F_{0dg}) && (2.21)\\
dL_{ug} &= F_{0tg} + 2\sigma\epsilon_w T_w^4 \frac{\text{skyw}}{\pi}(1 - V_{uc})\frac{kh_0}{b_w\frac{(1-V_{uc})}{V_{uc}}} && (2.22)\\
uL_{ug} &= \sigma\varepsilon_{ug}T_{ug}^4(1 - V_{uc}) && (2.23)\\
Rn_{ug} &= dS_{ug} + dL_{ug} - uS_{ug} - uL_{ug} && (2.24)
\end{aligned}
$$

2.2.5 Upward radiation from street canyon

Some of the incident radiation is reflected by reflectance (α). And, as mentioned above, some of the reflected radiation from wall and road will be received again by another element, and the rest of the reflected radiation will return to the sky. The partitioning of these radiations is described in **2.2.3** and **2.2.4**. The total of these returned radiations is upward short-wave radiation from the street canyon to the sky (uS_m). Ratio of uS_m to incident radiation (above the roof level) is the bulk albedo of street canyon system (roof-wall-road union).

$$
uS_m = uS_r + (uS_{lw} + uS_{rw})\frac{\text{skyw}}{\pi} + \alpha_{ug}F_{0dg}\frac{\text{skyg}}{\pi} + \alpha_{ug}F_{0bg}\left(1 - \frac{\phi + \psi}{\pi}\right) \qquad (2.25)
$$

All the emitted long-wave radiation from roof will return to the sky. Long-wave radiation emitted from wall and road will return to the sky according to the sky-view factor ($skyw, skyg$). The total of these returned radiations is upward long-wave radiation from the street canyon to the sky (uL_m).

$$
uL_m = uL_r + 2uL_w\frac{\text{skyw}}{\pi} + uL_{ug}\frac{\text{skyg}}{\pi} \qquad (2.26)
$$

2.2.6 Total net radiation and upward radiation

The radiation components presented above are those for the k-story street canyon. If we consider the various height of canyon, the total radiation absorbed by roof, wall, and road and total upward radiation from canyon system should be integrated using the roof height distribution (fractional area of each canyon).

$$
\begin{aligned}
Rn_{r,total} &= \sum_{k=1}^{n} Rn_{r,k}r(k) \quad Rn_{w,total} = \sum_{k=1}^{n} Rn_{w,k}r(k) \quad Rn_{ug,total} = \sum_{k=1}^{n} Rn_{ug,k}r(k) && (2.27)\\
uS_{m,total} &= \sum_{k=1}^{n} uS_{m,k}r(k) \quad uL_{m,total} = \sum_{k=1}^{n} uL_{m,k}r(k) && (2.28)
\end{aligned}
$$

where

$$
\sum_{k=1}^{n} r(k) = 1 \qquad (2.29)
$$

2.3 Turbulent transfer process

In this section, aerodynamic resistences are formulated according to the assumed arrangement of roughness element (buildings) and turbulent transfer theory.

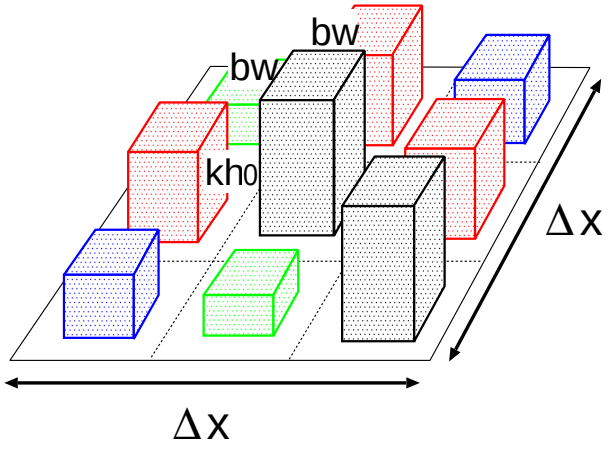

Figure 2.4: Arrangement of roughness element

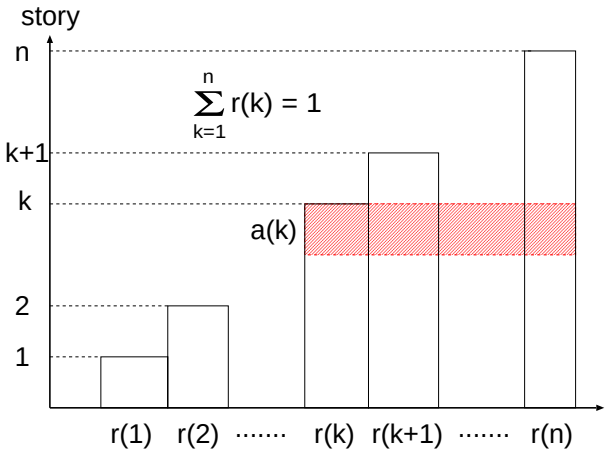

Figure 2.5: Roof height distribution

In the calculation of turbulent transfer process, each roughness element is expressed by a square prism (see **Figure 2.4**). All prisms are assumed to have the same width (b_w) and to be evenly spaced, while they have their own roof heights ($k\ h_0$ for k-story building).
For simplicity, $a(k)$ is defined as a total of roof height distribution ($r(k)$) from k-story to the top (n-story). And also A_b is defined as a total of roof height distribution ($r(k)$) multiplied by the height (k).

$$a(k) = \sum_{i=k}^{n} r(i) \tag{2.30}$$

$$A_b = \sum_{k=1}^{n} r(k)\ k \tag{2.31}$$

Where, $r(k)$ is fraction of k-story building.

$$\sum_{k=1}^{n} r(k) = 1 \tag{2.32}$$

If the horizontal scale of a grid area is Δx, total roof area of k-story buildings is $V_{uc} r(k) (\Delta x)^2$. While roof area of one building is b_w^2. Then number of k-story building is $V_{uc} r(k) (\frac{\Delta x}{b_w})^2$.
Therefore, total building frontal area per unit area (S_s) and total building surface area per unit area (S_r) are expressed as follows.

$$S_s = \sum_{k=1}^{n} b_w k\ h_0\ V_{uc} r(k) \left(\frac{\Delta x}{b_w}\right)^2 / (\Delta x)^2 = \left(\frac{h_0}{b_w}\right) V_{uc}\ A_b \tag{2.33}$$

$$S_r = V_{uc} + 4\ S_s \tag{2.34}$$

The building frontal area density in k-story layer per unit area ($A_s(k)$) is

$$A_s(k) = \sum_{i=k}^{n} b_w\ h_0\ V_{uc} r(k) \left(\frac{\Delta x}{b_w}\right)^2 / (\Delta x)^2 = \left(\frac{h_0}{b_w}\right) V_{uc}\ a(k) \tag{2.35}$$

2.3.1 Wind profile and momentum flux

As the density of roughness elements increases, so does the roughness (z_0) of the surface. But a point comes where adding new elements merely serves to reduce the effective drag of those already present due to mutual sheltering. As Shaw and Pereira (1982) note, at this point the increase in drag is offset by an increase in zero-plane displacement (d_0) (Grimmond et al. (1999)).
The dependence of z_0 and d_0 on the size, shape, density, and distribution of surface elements has been studied using wind tunnels, analytical investigations, and field observation.
In this model, we use a formulation of z_0 and d_0 following Macdonald et al. (1998). In their formula, both horizontal fraction of roughness element (plan area density) and vertical section (frontal area density) are considered. In our model, we replace frontal area density with total building frontal area per unit area (S_s) and roughness height with mean building height (z_{ave}).

$$z_{ave} = A_b h_0 \tag{2.36}$$

$$d_0 = z_{ave}\left[1 + 4.43^{-V_{uc}}(V_{uc} - 1)\right] \tag{2.37}$$

$$z_0 = (z_{ave} - d_0)\exp\left(-\left[0.5\frac{C_d}{\kappa^2}\left(1 - \frac{d_0}{z_{ave}}\right)S_s\right]^{-0.5}\right) \tag{2.38}$$

Assuming that the wind speed profile within canopy air space follows the exponential function by an attenuation coefficient a_w, wind speed at the k-story layer ($u(k)$) is expressed as follows.

$$u(k) = u_2 \exp\left[-a_w\left(1 - \frac{k}{n}\right)\right] \tag{2.39}$$

Where u_2 is wind speed at the top of the canopy ($z = z_2 = nh_0$). According to Macdonald (2000), a_w can be approximated by linear relationship with frontal area density ($a_w = 9.6S_s$).
As a first guess, we assume a neutral condition for describing the log-linear profile of wind speed above the canopy. Then, a friction velocity (u_*) and u_2 are obtained from u_m.

$$u_* = \frac{\kappa u_m}{\ln\left(\frac{z_m - d_0}{z_0}\right)} \tag{2.40}$$

$$u_2 = \frac{u_*}{\kappa}\ln\left(\frac{z_2 - d_0}{z_0}\right) \tag{2.41}$$

As for the profile of vertical eddy diffusivity (K_m), it is propotional to the height in log-linear region (above canopy). And K_m is propotional to the local wind speed within canopy.

$$K_m(k) = \kappa u_*(kh_0 - d_0) \qquad (k \geq n) \tag{2.42}$$

$$K_m(k) = \eta u(k) \qquad (k \leq n) \tag{2.43}$$

η is obtained from the continuity of K_m at canopy top height ($k = n$).

$$\eta = \frac{\kappa u_*(nh_0 - d_0)}{u_2} \tag{2.44}$$

2.3.2 Aerodynamic resistance

Now aerodynamic resistances (r_r, r_w, r_{du}, and r_{au}) can be calculated using the profiles of u and K_m. Transfer pathways of sensible heat in the urban canopy model are shown in **Figure 2.6**.

1. from the roof to the canyon air space (r_r)

2. from the wall to the canyon air space (r_w)

3. from the road to the canyon air space (r_{du})

4. from the canyon air space to the reference level (r_{au})

In case of urban canopy, wall (frontal area) is important for momentum absorption, and roof (surface area) is so for scalar (heat and water vapor) transfer. In case of vegetation canopy, leaf is important for both momentum and scalar transfer. This is a fundamental difference between urban canopy and vegetation canopy.
Thus, in calculating bulk aerodynamic resistances of roof and wall, surface area densities ($A_{rr}(k)$, $A_{rw}(k)$) are used instead of frontal area density ($A_s(k)$).

$$\frac{1}{r_r} = \sum_{k=1}^{n} \frac{A_{rr}(k)\sqrt{U(k)}}{p_s\ C_s} h_0 = \frac{V_{uc}}{p_s\ C_s} \sum_{k=1}^{n} \left(r(k)\sqrt{U(k)} \right) \tag{2.45}$$

$$\frac{1}{r_w} = \sum_{k=1}^{n} \frac{A_{rw}(k)\sqrt{U(k)}}{p_s\ C_s} h_0 = \frac{4V_{uc}}{p_s\ C_s} \left(\frac{h_0}{b_w} \right) \sum_{k=1}^{n} \left(a(k)\sqrt{U(k)} \right) \tag{2.46}$$

The extent to which the drag on individual roughness elements is reduced by the presence of neighbours was expressed by Thom (1971) in terms of a shelter factor. But shelter factor (p_s) is still not well understood. It accounts for the observation that the drag coefficient of an ensemble of roughness elements is less than the sum of their individual drag coefficients, presumably due to mutual sheltering effects. Using the same relationship as the case for vegetation canopy, p_s is expressed by power function, exept that leaf area density is replaced by frontal area density.

$$p_s = 1 + \left(\frac{S_s}{nh_0} \right)^{0.6} = 1 + \left(\frac{V_{uc} A_b}{n b_w} \right)^{0.6} \tag{2.47}$$

This relationship should be investigated for the array of different height of roughness elements.
The road to canopy air space resistance (r_{du}) is defined as follows.

$$r_{du} = \int_0^{h_a} \frac{1}{K_m} dz = \sum_{k=1}^{k_{ha}} \frac{h_0}{K_m(k)} \tag{2.48}$$

Canopy source height ($h_a = k_{ha} h_0$) is assumed to be equal to the center of action of r_r and r_w within the canopy as obtained from the solution of

$$\sum_{k=1}^{k_{ha}} \left(r(k) + 4 \left(\frac{h_0}{b_w} \right) a(k) \right) \sqrt{U(k)} \simeq \sum_{k=k_{ha}}^{n} \left(r(k) + 4 \left(\frac{h_0}{b_w} \right) a(k) \right) \sqrt{U(k)} \tag{2.49}$$

Resistance between canopy air space and reference height (r_{au}) can be described by integration of K_m over the distance from h_a to z_m.

$$r_{au} = \int_{h_a}^{nh_0} \frac{1}{K_m} dz + \int_{nh_0}^{z_m} \frac{1}{K_m} dz = \sum_{k=k_{ha}}^{n} \frac{h_0}{K_m(k)} + \frac{1}{\kappa u_*} \ln \left(\frac{z_m - d_0}{nh_0 - d_0} \right) \tag{2.50}$$

Above formulation is based on the neutral condition. The nonneutral adjustment to aerodynamic resistances is executed according to Monin-Obukov similarity (see next section).

2.4 Sensible heat flux

If we assume no storage of heat at any of the junctions of the resistance network shown in **Figure 2.6**, we can write the area-averaged sensible heat fluxes from the roof, wall, and road as follows.

$$H_r = A(T_r - T_{au}), \qquad A = \rho_a C_p / r_r \tag{2.51}$$
$$H_w = B(T_w - T_{au}), \qquad B = \rho_a C_p / r_w \tag{2.52}$$
$$H_{ug} = C(T_{ug} - T_{au}), \qquad C = \rho_a C_p / r_{du} \tag{2.53}$$
$$H_r + H_w + H_{ug} = D(T_{au} - T_m), \qquad D = \rho_a C_p / r_{au} \tag{2.54}$$

Canyon air space temperature (T_{au}) can be eliminated by asuuming that energy fluxes from roof, wall, and road are all transfered to atmospheric boundary layer, in another word, no energy is stored in canopy air space.

$$T_{au} = \frac{A \cdot T_r + B \cdot T_w + C \cdot T_{ug} + D \cdot T_m}{A + B + C + D} \tag{2.55}$$

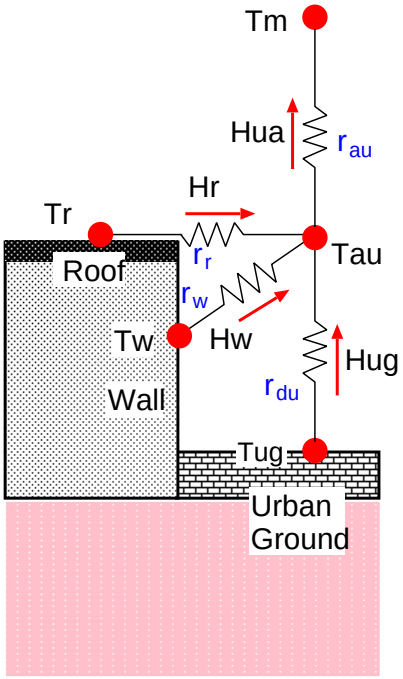

Figure 2.6: Transfer pathways of sensible heat flux and aerodynamic resistances

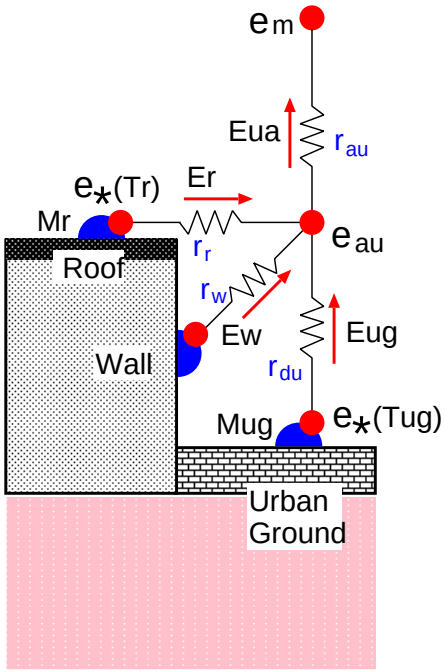

Figure 2.7: Transfer pathways of latent heat flux and aerodynamic resistances

Now atmospheric stability can be calculated from the temperature difference between canyon air space and reference height ($T_{au} - T_m$).

$$H = \rho_a C_p (T_{au} - T_m) \kappa u_* / \Psi_H \tag{2.56}$$
$$L = -\rho_a C_p T_m u_*^3 / \kappa g H \tag{2.57}$$
$$\zeta = z_m / L \tag{2.58}$$

In the urban area, sensible heat flux is usually dominant to latent heat flux. Therefore, only sensible heat flux is considered in **eq.(2.57)**. If ζ is not close to zero, wind profile used in the previous section should be modified by integrated universal function.

when $\zeta < 0$ (unstable)

$$\Psi_M = \ln\left(\frac{z_m - d_0}{z_0}\right) + \ln\frac{(x_0^2+1)(x_0+1)^2}{(x^2+1)(x+1)^2} + 2(\tan^{-1}x - \tan^{-1}x_0) \tag{2.59}$$

$$\Psi_H = \ln\left(\frac{z_m - d_0}{z_0}\right) + 2\ln\left(\frac{y_0+1}{y+1}\right) \tag{2.60}$$

$$x = (1-16\zeta)^{1/4},\ x_0 = (1-16\zeta_0)^{1/4},\ y = (1-16\zeta)^{1/2},\ y_0 = (1-16\zeta_0)^{1/2} \tag{2.61}$$

when $\zeta \geq 0$ (stable)

$$\Psi_M = \ln\left(\frac{z_m - d_0}{z_0}\right) + \frac{7}{3}\ln\frac{1+3\zeta+10\zeta^3}{1+3\zeta_0+10\zeta_0^3} \tag{2.62}$$

$$\Psi_H = \ln\left(\frac{z_m - d_0}{z_0}\right) + 400\ln\frac{1+7/400\zeta+0.005\zeta^2}{1+7/400\zeta_0+0.005\zeta_0^2} \tag{2.63}$$

$$u_* = \kappa u_m/\Psi_M \tag{2.64}$$

Now u_* from **eq.(2.40)** (neutral value) is replaced by u_* from **eq.(2.64)** (nonneutral value), and go back to **eq.(2.41)**. The above procedure is repeated until convergence condition (in ζ) is obtained. Note that Ψ_H in **eq.(2.56)** is equal to $\ln\left(\frac{z_m-d_0}{z_0}\right)$ for the first iteration step.

2.5 Rainfall interception and interception loss

The interception of rainfall and evaporation of intercepted water is modeled very simply. Basically, each components of urban canopy model (roof, wall, road) is assumed to be impermeable. And, different from the case for vegetation, roof is only one layer (interception area is much smaller than vegetation canopy).

The maximum values for water store (S_i) are set to each story. If the water store (M_i) exceeds the maximum value, the drainage (D_i) occurs.

$$P_r = P\,V_{uc} \tag{2.65}$$

$$D_r = \begin{cases} = 0 & \text{when} \quad M_r < S_r \\ = P_r & \text{when} \quad M_r = S_r \end{cases} \tag{2.66}$$

$$P_w = D_r \tag{2.67}$$

$$D_w = \begin{cases} = 0 & \text{when} \quad M_w < S_w \\ = D_r & \text{when} \quad M_w = S_w \end{cases} \tag{2.68}$$

$$P_{ug} = P\,(1-V_{uc}) + D_w \tag{2.69}$$

$$D_{ug} = \begin{cases} = 0 & \text{when} \quad M_{ug} < S_{ug} \\ = P_{ug} & \text{when} \quad M_{ug} = S_{ug} \end{cases} \tag{2.70}$$

D_{ug} is the surface runoff from urban area. It will flow into water body, or it will be used as input of runoff model.

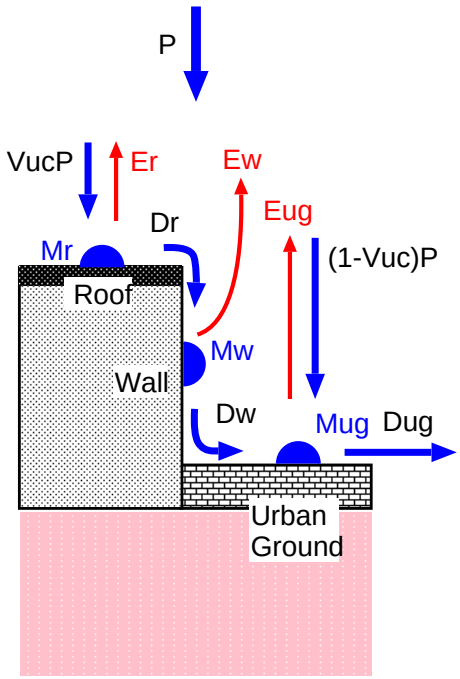

Figure 2.8: Rainfall interception model

The quantities M_r, M_w, M_{ug} are used to determine the fractional wetted areas of the roof, wall, and road (W_r, W_w, W_{ug}). So the rates of evaporation from the wetted portions of the roof, wall, and road are expressed as follows.

$$\lambda E_r = E[e_*(T_r) - e_{au}], \qquad E = \frac{\rho_a C_p}{\gamma}\frac{W_r}{r_r} \tag{2.71}$$

$$\lambda E_w = F[e_*(T_w) - e_{au}], \qquad F = \frac{\rho_a C_p}{\gamma}\frac{W_w}{r_w} \tag{2.72}$$

$$\lambda E_{ug} = G[e_*(T_{ug}) - e_{au}], \qquad G = \frac{\rho_a C_p}{\gamma}\frac{W_{ug}}{r_{du}} \tag{2.73}$$

$$\lambda E_r + \lambda E_w + \lambda E_{ug} = H[e_*(e_{au}) - e_m], \qquad H = \frac{\rho_a C_p}{\gamma}\frac{W_r}{r_{au}} \tag{2.74}$$

$$\tag{2.75}$$

e_{au} can be eliminated by asuuming that water vapor fluxes from roof, wall, and road are all transfered to atmospheric boundary layer, in another word, no water vapor is stored in canopy air space.

$$e_{au} = \frac{E \cdot e_*(T_r) + F \cdot e_*(T_w) + G \cdot e_*(T_{ug}) + H \cdot e_m}{E + F + G + H} \tag{2.76}$$

$$W_r = \begin{cases} = M_r/S_r & \text{when} \quad e_*(T_r) > e_{au} \\ = 1 & \text{when} \quad e_*(T_r) \le e_{au} \end{cases} \tag{2.77}$$

$$W_w = \begin{cases} = M_w/S_w & \text{when} \quad e_*(T_r) > e_{au} \\ = 1 & \text{when} \quad e_*(T_r) \le e_{au} \end{cases} \tag{2.78}$$

$$W_{ug} = \begin{cases} = M_{ug}/S_{ug} & \text{when} \quad e_*(T_{ug}) > e_{au} \\ = 1 & \text{when} \quad e_*(T_{ug}) \le e_{au} \end{cases} \tag{2.79}$$

$$\tag{2.80}$$

It is assumed in **eq.(2.71), (2.72), (2.73)** that wet and dry parts of the surface are at the same temperature. Basically, the maximum water storage is much smaller than vegetation canopy, and the duration time of water to present on the surface is very short, it is better to use the same temperature for wet and dry parts.

2.6 Prognostic variables and their governing equations

Urban canopy model has seven prognostic physical-state variables: four temperatures (for roof, T_r, for wall, T_w, for road, T_{ug}, and for under ground, T_{du}); three interception water stores (for roof, M_r, for wall, M_w, and for road M_{ug}). Where T_{du} is defined as mean value of T_{ug} over one day.

2.6.1 Governing equations for temperatures

The governing equations for the four temperatures are based on force-restore method (Bhumralkar, 1975; Blackadar, 1976). The force-restore approximation relies on the analytical solution of the heat conduction equation under periodic forcing, which is used to parameterize the almost periodic

daily ground heat flux. In this way, a very simple and efficient but reasonably accurate description of the temperature dynamics can be achieved.
In this model, prognostic equation for surface temperature incorporates both surface energy flux (atmospheric forcing term) and soil heat flux (restoring term) to reproduce the diurnal variation of surface temperature realistically.
In case of the urban canopy model, three surface temperatures (T_r, T_w, T_{ug}) are predicted. As for the restoring term for T_r and T_w, a inner building temperature (T_{bi}), which may be controlled or maintained by human activity, is used. Furthermore, artificial heat source (Q_m [1]), which is a result of human activity, is added to the forcing term. So, the prognostic equations for temperatures in urban canopy model are expressed as follows.

$$C_r\frac{\partial T_r}{\partial t} = Rn_r - H_r - \lambda E_r - \omega C_r(T_r - T_{bi}) + Q_m V_{uc} \tag{2.81}$$
$$C_w\frac{\partial T_w}{\partial t} = Rn_w - H_w - \lambda E_w - \omega C_w(T_w - T_{bi}) + Q_m A_w \tag{2.82}$$
$$C_{ug}\frac{\partial T_{ug}}{\partial t} = Rn_{ug} - H_{ug} - \lambda E_{ug} - \omega C_{ug}(T_{ug} - T_{du}) + Q_m(1 - V_{uc}) \tag{2.83}$$
$$C_{du}\frac{\partial T_{du}}{\partial t} = Rn_{ug} - H_{ug} - \lambda E_{ug} - \omega C_{du}(T_{du} - T_{bi}) + Q_m(1 - V_{uc}) \tag{2.84}$$

The effective heat capacities (C_r, C_w, C_{ug}, C_{du}) are defined theoretically using specific heat and thermal conductivity.

$$C_i = \left(\frac{c_i k_i}{2\omega}\right)^{1/2} \qquad \text{(i=r,w,ug)} \tag{2.85}$$
$$C_{du} = \sqrt{365}C_{ug} \tag{2.86}$$

where

Q_m = anthropogenic heat source ($\mathrm{Wm^{-2}}$)
$C_i(i = r, w, ug, du)$ = effective heat capacity ($\mathrm{J\ m^{-2}K^{-1}}$)

As for **eq. (2.86)**, heat capacity is propotional to a square root of cycle. T_{du} is defined as mean value of T_{ug} over one day, and T_{du} is expected to have seasonal cycle (one year).
Effective heat capacity is impotant for reproducing the amplitude and phase of diurnal cycle. Basically, actual values of thermal properties (c_i, k_i) are dependent on material (concrete, asphalt, tile, etc.). In practice, these parameters are adjusted to reproduce the diurnal cycle, since urban canopy consists of different kinds of materials.

2.6.2 Governing equations for intercepted water

The governing equations for the three interception water stores are expressed in the same formula.

$$\frac{\partial M_i}{\partial t} = P_i - D_i - \frac{E_i}{\rho_w} \qquad \text{(i = r, w, ug)} \tag{2.87}$$

This is simple water budget equation for water store. In the calculation of water store (M_i), evaporation (E_i) is modified if **eq.(2.87)** produces a negative value of M_i.

[1] Usually, T_{bi} is controlled by air conditioner. Then, Q_m should be related to T_{bi} or temperature difference with outside ($T_{bi} - T_m$). Furthermore, additional energy will be released as a result of domestic use. There is no good way to formulate T_{bi} and Q_m at present. Therefore, they are treated as parameter (prescribed, changable with time). The role of Q_m will be discussed in the later section (see **??**).

2.7 Numerical solution of prognostic equations

In the numerical solution of the prognostic equations for temperatures (T_r, T_w, T_{ug}), we make use of the fact that the storage terms, involving $C_i (i = r, w, ug)$, are small relative to the energy fluxes $Rn_i, \lambda E_i, and H_i (i = r, w, ug)$. These values make **eq. (2.81), (2.82), (2.83)** fast response equations so that changes in T_r, T_w, T_{ug}, even over a time step as short as an hour, can have a significant feedback on the magnitude of the energy fluxes. The energy fluxes are explicit functions of atmospheric boundary conditions, prognostic variables, and aerodynamic resistances. Prognostic equations are solved by an implicit backward method using partial derivatives of each term.

First, considering the energy fluxes in prognostic equations are functions of temperature, partial derivatives are calculated in subroutine **partial**. Then, prognostic equations are expressed in explicit backward-differencing form and a set of linear simultaneous equations regarding the changes in temperatures over a time step (Δt) are obtained.

Not only energy fluxes but also heat exchange terms have dependency on temperatures. Now prognostic equations can be written in discrete-time form.

$$\begin{aligned}
C_r\frac{\Delta T_r}{\Delta t} &= Rn_r - H_r - \lambda E_r - \omega C_r(T_r - T_{bi}) + Q_m V_{uc} \\
&\quad + \frac{\partial Rn_r}{\partial T_r}\Delta T_r - (\frac{\partial H_r}{\partial T_r}\Delta T_r + \frac{\partial H_r}{\partial T_w}\Delta T_w + \frac{\partial H_r}{\partial T_{ug}}\Delta T_{ug}) \\
&\quad - (\frac{\partial \lambda E_r}{\partial T_r}\Delta T_r + \frac{\partial \lambda E_r}{\partial T_w}\Delta T_w + \frac{\partial \lambda E_r}{\partial T_{ug}}\Delta T_{ug}) - \omega C_r \Delta T_r \qquad (2.88) \\
C_w\frac{\Delta T_w}{\Delta t} &= Rn_w - H_w - \lambda E_w - \omega C_w(T_w - T_{bi}) + Q_m A_w \\
&\quad + (\frac{\partial Rn_w}{\partial T_w}\Delta T_w + \frac{\partial Rn_w}{\partial T_{ug}}\Delta T_{ug}) - (\frac{\partial H_w}{\partial T_w}\Delta T_w + \frac{\partial H_w}{\partial T_r}\Delta T_r + \frac{\partial H_w}{\partial T_{ug}}\Delta T_{ug}) \\
&\quad - (\frac{\partial \lambda E_w}{\partial T_w}\Delta T_w + \frac{\partial \lambda E_w}{\partial T_r}\Delta T_r + \frac{\partial \lambda E_w}{\partial T_{ug}}\Delta T_{ug}) - \omega C_w \Delta T_w \qquad (2.89) \\
C_{ug}\frac{\Delta T_{ug}}{\Delta t} &= Rn_{ug} - H_{ug} - \lambda E_{ug} - \omega C_{ug}(T_{ug} - T_{du}) + Q_m(1 - V_{uc}) \\
&\quad + (\frac{\partial Rn_{ug}}{\partial T_{ug}}\Delta T_{ug} + \frac{\partial Rn_{ug}}{\partial T_w}\Delta T_w) - (\frac{\partial H_{ug}}{\partial T_{ug}}\Delta T_{ug} + \frac{\partial H_{ug}}{\partial T_r}\Delta T_r + \frac{\partial H_{ug}}{\partial T_w}\Delta T_w) \\
&\quad - (\frac{\partial \lambda E_{ug}}{\partial T_{ug}}\Delta T_{ug} + \frac{\partial \lambda E_{ug}}{\partial T_r}\Delta T_r + \frac{\partial \lambda E_{ug}}{\partial T_w}\Delta T_w) - \omega C_{ug}(\Delta T_{ug} - \Delta T_{du}) \qquad (2.90) \\
C_{du}\frac{\Delta T_{du}}{\Delta t} &= Rn_{ug} - H_{ug} - \lambda E_{ug} + \omega C_{du}(T_{bi} - T_{du}) + Q_m(1 - V_{uc}) \\
&\quad + (\frac{\partial Rn_{ug}}{\partial T_{ug}}\Delta T_{ug} + \frac{\partial Rn_{ug}}{\partial T_w}\Delta T_w) - (\frac{\partial H_{ug}}{\partial T_{ug}}\Delta T_{ug} + \frac{\partial H_{ug}}{\partial T_r}\Delta T_r + \frac{\partial H_{ug}}{\partial T_w}\Delta T_w) \\
&\quad - (\frac{\partial \lambda E_{ug}}{\partial T_{ug}}\Delta T_{ug} + \frac{\partial \lambda E_{ug}}{\partial T_r}\Delta T_r + \frac{\partial \lambda E_{ug}}{\partial T_w}\Delta T_w) - \omega C_{du}\Delta T_{du} \qquad (2.91)
\end{aligned}$$

If it is written in matrix form,

$$KX = Y \qquad \longrightarrow \qquad X = K^{-1}Y$$

$$K = \begin{bmatrix} K_{1,1} & K_{1,2} & K_{1,3} & K_{1,4} \\ K_{2,1} & K_{2,2} & K_{2,3} & K_{2,4} \\ K_{3,1} & K_{3,2} & K_{3,3} & K_{3,4} \\ K_{4,1} & K_{4,2} & K_{4,3} & K_{4,4} \end{bmatrix} \qquad X = \begin{bmatrix} \Delta T_r \\ \Delta T_w \\ \Delta T_{ug} \\ \Delta T_{du} \end{bmatrix}$$

where

$$
\begin{array}{ll}
K_{1,1} = \frac{C_r}{\Delta t} - \frac{\partial Rn_r}{\partial T_r} + \frac{\partial H_r}{\partial T_r} + \frac{\partial \lambda E_r}{\partial T_r} + \omega C_r & K_{1,2} = \frac{\partial H_r}{\partial T_w} + \frac{\partial \lambda E_r}{\partial T_w} \\
K_{1,3} = \frac{\partial H_r}{\partial T_{ug}} + \frac{\partial \lambda E_r}{\partial T_{ug}} & K_{1,4} = 0 \\
K_{2,1} = \frac{\partial H_w}{\partial T_r} + \frac{\partial \lambda E_w}{\partial T_r} & K_{2,2} = \frac{C_w}{\Delta t} - \frac{\partial Rn_w}{\partial T_w} + \frac{\partial H_w}{\partial T_w} + \frac{\partial \lambda E_w}{\partial T_w} + \omega C_w \\
K_{2,3} = -\frac{\partial Rn_w}{\partial T_{ug}} + \frac{\partial H_w}{\partial T_{ug}} + \frac{\partial \lambda E_w}{\partial T_{ug}} & K_{2,4} = 0 \\
K_{3,1} = \frac{\partial H_{ug}}{\partial T_r} + \frac{\partial \lambda E_{ug}}{\partial T_r} & K_{3,2} = -\frac{\partial Rn_{ug}}{\partial T_w} + \frac{\partial H_{ug}}{\partial T_w} + \frac{\partial \lambda E_{ug}}{\partial T_w} \\
K_{3,3} = \frac{C_{ug}}{\Delta t} - \frac{\partial Rn_{ug}}{\partial T_{ug}} + \frac{\partial H_{ug}}{\partial T_{ug}} + \frac{\partial \lambda E_{ug}}{\partial T_{ug}} + \omega C_{ug} & K_{3,4} = -\omega C_g \\
K_{4,1} = \frac{\partial H_{ug}}{\partial T_r} + \frac{\partial \lambda E_{ug}}{\partial T_r} & K_{4,2} = -\frac{\partial Rn_{ug}}{\partial T_w} + \frac{\partial H_{ug}}{\partial T_w} + \frac{\partial \lambda E_{ug}}{\partial T_w} \\
K_{4,3} = -\frac{\partial Rn_{ug}}{\partial T_{ug}} + \frac{\partial H_{ug}}{\partial T_{ug}} + \frac{\partial \lambda E_{ug}}{\partial T_{ug}} & K_{4,4} = \frac{C_{du}}{\Delta t} + \omega C_{du}
\end{array}
$$

$$
Y = \begin{bmatrix}
Rn_r - H_r - \lambda E_r - \omega C_r (T_r - T_{bi}) + Q_m V_{uc} \\
Rn_w - H_w - \lambda E_w - \omega C_w (T_w - T_{bi}) + Q_m A_w \\
Rn_g - H_{ug} - \lambda E_{ug} - \omega C_{ug} (T_{ug} - T_{du}) + Q_m (1 - V_{uc}) \\
Rn_g - H_{ug} - \lambda E_{ug} + \omega C_{du} (T_{bi} - T_{du}) + Q_m (1 - V_{uc})
\end{bmatrix}
$$

Above equations can be solved in terms of temperature changes $(\Delta T_r, \Delta T_w, \Delta T_{ug}, \Delta T_{du})$. Each temperatures are updated to the value at time $t_0 + \Delta t$ by adding temperature changes to the initial value at time t_0. Furthermore, energy fluxes are modified to show the values averaged over a time step (between time t_0 and time $t_0 + \Delta t$).

$$
\begin{aligned}
Rn'_r &= Rn_r + \frac{1}{2} \frac{\partial Rn_r}{\partial T_r} \Delta T_r && (2.92) \\
Rn'_w &= Rn_w + \frac{1}{2} (\frac{\partial Rn_w}{\partial T_w} \Delta T_w + \frac{\partial Rn_w}{\partial T_{ug}} \Delta T_{ug}) && (2.93) \\
Rn'_g &= Rn_g + \frac{1}{2} (\frac{\partial Rn_{ug}}{\partial T_w} \Delta T_w + \frac{\partial Rn_{ug}}{\partial T_{ug}} \Delta T_{ug}) && (2.94) \\
H'_r &= H_r + \frac{1}{2} (\frac{\partial H_r}{\partial T_r} \Delta T_r + \frac{\partial H_r}{\partial T_w} \Delta T_w + \frac{\partial H_r}{\partial T_{ug}} \Delta T_{ug}) && (2.95) \\
H'_w &= H_w + \frac{1}{2} (\frac{\partial H_w}{\partial T_r} \Delta T_r + \frac{\partial H_w}{\partial T_w} \Delta T_w + \frac{\partial H_w}{\partial T_{ug}} \Delta T_{ug}) && (2.96) \\
H'_g &= H_g + \frac{1}{2} (\frac{\partial H_{ug}}{\partial T_r} \Delta T_r + \frac{\partial H_{ug}}{\partial T_w} \Delta T_w + \frac{\partial H_{ug}}{\partial T_{ug}} \Delta T_{ug}) && (2.97) \\
\lambda E'_r &= \lambda E_r + \frac{1}{2} (\frac{\partial \lambda E_r}{\partial T_r} \Delta T_r + \frac{\partial \lambda E_r}{\partial T_w} \Delta T_w + \frac{\partial \lambda E_r}{\partial T_{ug}} \Delta T_{ug}) && (2.98) \\
\lambda E'_w &= \lambda E_w + \frac{1}{2} (\frac{\partial \lambda E_w}{\partial T_r} \Delta T_r + \frac{\partial \lambda E_w}{\partial T_w} \Delta T_w + \frac{\partial \lambda E_w}{\partial T_{ug}} \Delta T_{ug}) && (2.99) \\
\lambda E'_{ug} &= \lambda E_{ug} + \frac{1}{2} (\frac{\partial \lambda E_{ug}}{\partial T_r} \Delta T_r + \frac{\partial \lambda E_{ug}}{\partial T_w} \Delta T_w + \frac{\partial \lambda E_{ug}}{\partial T_{ug}} \Delta T_{ug}) && (2.100)
\end{aligned}
$$

Following **Section 2.2**, five partial derivatives of net radiation fluxes (Rn_r, Rn_w, Rn_{ug}) are obtained as follows.

$$\frac{\partial Rn_r}{\partial T_r} = -4\sigma\varepsilon_r T_r^3 V_{uc} \tag{2.101}$$

$$\frac{\partial Rn_w}{\partial T_w} = 4\sigma\varepsilon_w T_w^3 \frac{\pi - 2\text{skyw}}{\pi}(1-V_{uc}) \sum_{k=1}^{n} \frac{kh_0}{b_w \frac{(1-V_{uc})}{V_{uc}}} - 4\sigma\varepsilon_w T_w^3 (1-V_{uc}) \sum_{k=1}^{n} \frac{kh_0}{b_w \frac{(1-V_{uc})}{V_{uc}}} \tag{2.102}$$

$$\frac{\partial Rn_w}{\partial T_g} = 4\sigma\varepsilon_g T_g^3 \frac{\pi - \text{skyg}}{2\pi}(1-V_{uc}) \tag{2.103}$$

$$\frac{\partial Rn_{ug}}{\partial T_{ug}} = -4\sigma\varepsilon_{ug} T_{ug}^3 (1-V_{uc}) \tag{2.104}$$

$$\frac{\partial Rn_{ug}}{\partial T_w} = 8\sigma\varepsilon_w T_w^3 \frac{\text{skyw}}{\pi}(1-V_{uc}) \sum_{k=1}^{n} \frac{kh_0}{b_w \frac{(1-V_{uc})}{V_{uc}}} \tag{2.105}$$

Following **Section 2.4**, nine partial derivatives of sensible heat fluxes (H_r, H_w, H_{ug}) are obtained as follows.

$$T_{au} = \frac{A \cdot T_r + B \cdot T_w + C \cdot T_{ug} + D \cdot T_m}{A+B+C+D} \tag{2.106}$$

$$\frac{\partial H_r}{\partial T_r} = \frac{A(B+C+D)}{A+B+C+D}, \quad \frac{\partial H_r}{\partial T_w} = \frac{-AB}{A+B+C+D}, \quad \frac{\partial H_r}{\partial T_{ug}} = \frac{-AC}{A+B+C+D} \tag{2.107}$$

$$\frac{\partial H_w}{\partial T_w} = \frac{B(A+C+D)}{A+B+C+D}, \quad \frac{\partial H_w}{\partial T_r} = \frac{-AB}{A+B+C+D}, \quad \frac{\partial H_w}{\partial T_{ug}} = \frac{-BC}{A+B+C+D} \tag{2.108}$$

$$\frac{\partial H_{ug}}{\partial T_{ug}} = \frac{C(A+B+D)}{A+B+C+D}, \quad \frac{\partial H_{ug}}{\partial T_r} = \frac{-AC}{A+B+C+D}, \quad \frac{\partial H_{ug}}{\partial T_w} = \frac{-BC}{A+B+C+D} \tag{2.109}$$

Following **Section 2.5**, nine partial derivatives of latent heat fluxes ($\lambda E_r, \lambda E_w, \lambda E_{ug}$) are obtained as follows. Where, $e'_*(T_i)$ is a slope of saturation vapor pressure curve at T_i.

$$e_{au} = \frac{E \cdot e_*(T_r) + F \cdot e_*(T_w) + G \cdot e_*(T_{ug}) + H \cdot e_m}{E+F+G+H} \tag{2.110}$$

$$\frac{\partial \lambda E_r}{\partial T_r} = \frac{e'_*(T_r)E(F+G+H)}{E+F+G+H}, \quad \frac{\partial \lambda E_r}{\partial T_w} = \frac{-e'_*(T_w)EF}{E+F+G+H}, \quad \frac{\partial \lambda E_r}{\partial T_{ug}} = \frac{-e'_*(T_{ug})EG}{E+F+G+H} \tag{2.111}$$

$$\frac{\partial \lambda E_w}{\partial T_w} = \frac{e'_*(T_w)F(E+G+H)}{E+F+G+H}, \quad \frac{\partial \lambda E_w}{\partial T_r} = \frac{-e'_*(T_r)EF}{E+F+G+H}, \quad \frac{\partial \lambda E_w}{\partial T_{ug}} = \frac{-e'_*(T_{ug})FG}{E+F+G+H} \tag{2.112}$$

$$\frac{\partial \lambda E_{ug}}{\partial T_{ug}} = \frac{e'_*(T_{ug})G(E+F+H)}{E+F+G+H}, \quad \frac{\partial \lambda E_{ug}}{\partial T_r} = \frac{-e'_*(T_r)EG}{E+F+G+H}, \quad \frac{\partial \lambda E_{ug}}{\partial T_w} = \frac{-e'_*(T_w)FG}{E+F+G+H} \tag{2.113}$$

Chapter 3

Water Body model

In this chapter, water body model to be used as sub-model of land-surface scheme is formulated based on force-restore model. A dataset from flux measurement system of the Lake Biwa Project (see **Appendix ??**) is used for the development and validation of the water body model. Performance of the produced model is also shown by numerical simulaton. Variables and parameters used in this chapter are listed in **Table 3.1**. Physical constants are listed in **Table A.1** in **Appendix A**.

Table 3.1: Variables and parameters in the water body model

symbol	definition	unit
z_m	reference height	m
u_m	wind speed at reference height	m s^{-1}
T_m	air temperature at reference height	K
e_m	vapor pressure at reference height	mb
q_m	specific humidity at reference height	kg kg^{-1}
μ	cosine of zenith angle of incident beam	
T_{wb}	temperature of surface layer	K
T_{dw}	temperature of deep layer	K
q_{wb}	saturation specific humidity at T_{wb}	kg kg^{-1}
Rn_{wb}	net radiation flux	W m^{-2}
$F_{s,wb}$	short-wave radiation absorbed by water body	W m^{-2}
H_{wb}	sensible heat flux	W m^{-2}
E_{wb}	evaporation rate	kg $m^{-2}S^{-1}$
τ_{wb}	momentum flux absorbed by water surface	kg $m^{-1}s^{-2}$
u_*	friction velocity	m s^{-1}
z_0	surface roughness	m
L	Monin-Obukov length	m
ζ	non-dimensional stability factor	
r_{aw}	aerodynamic resistance between water surface and reference height	s m^{-1}
C_{wb}	effective heat capacity of surface layer	$J\ m^{-2}K^{-1}$
C_{dw}	effective heat capacity of deep layer	J $m^{-2}K^{-1}$
Z_s	effective depth of surface layer	m
β	short-wave radiation penetration factor	
α	albedo of water surface	
α_1, α_2	parameter for albedo model ($\alpha = \alpha_1 \mu^{\alpha_2}$)	

3.1 Energy balance at water surface

Figure 3.1 shows an example of seasonal variation of energy budget at the Lake Biwa in Japan. Horizontal axis is time (day) from 25th July in 1999 to 24th July in 2000. Upper figure is a time series of daily data, and lower one is a moving average of 15 days.
The net radiation (Rn) has its maximum in July and minimum (nearly zero) in December. Very small net radiation in December can be explained by small sunshine and large upward long-wave radiation. Observation site is located at the north part of the Lake Biwa. Then, sunshine is small (almost cloudy) in winter season. Furthermore, due to the relatively warm temperature, upward long-wave radiation is larger than downward.
In spite of much net radiative energy, latent heat (evaporation) is not so large from early spring to late summer. On the other hand, latent heat (evaporation) is large (even larger than net radiation) during autumn and winter season.
What I want to say here is that there is a phase lag between seasonal cycle of net radiation (Rn), latent heat (λE), and sensible heat (H). This means that significant part of energy is not used (or released) in a diurnal cycle of energy budget, and handed over in a seasonal cycle. This kind of seasonal dynamics of energy budget is peculiar to water body, especially in deep lake.

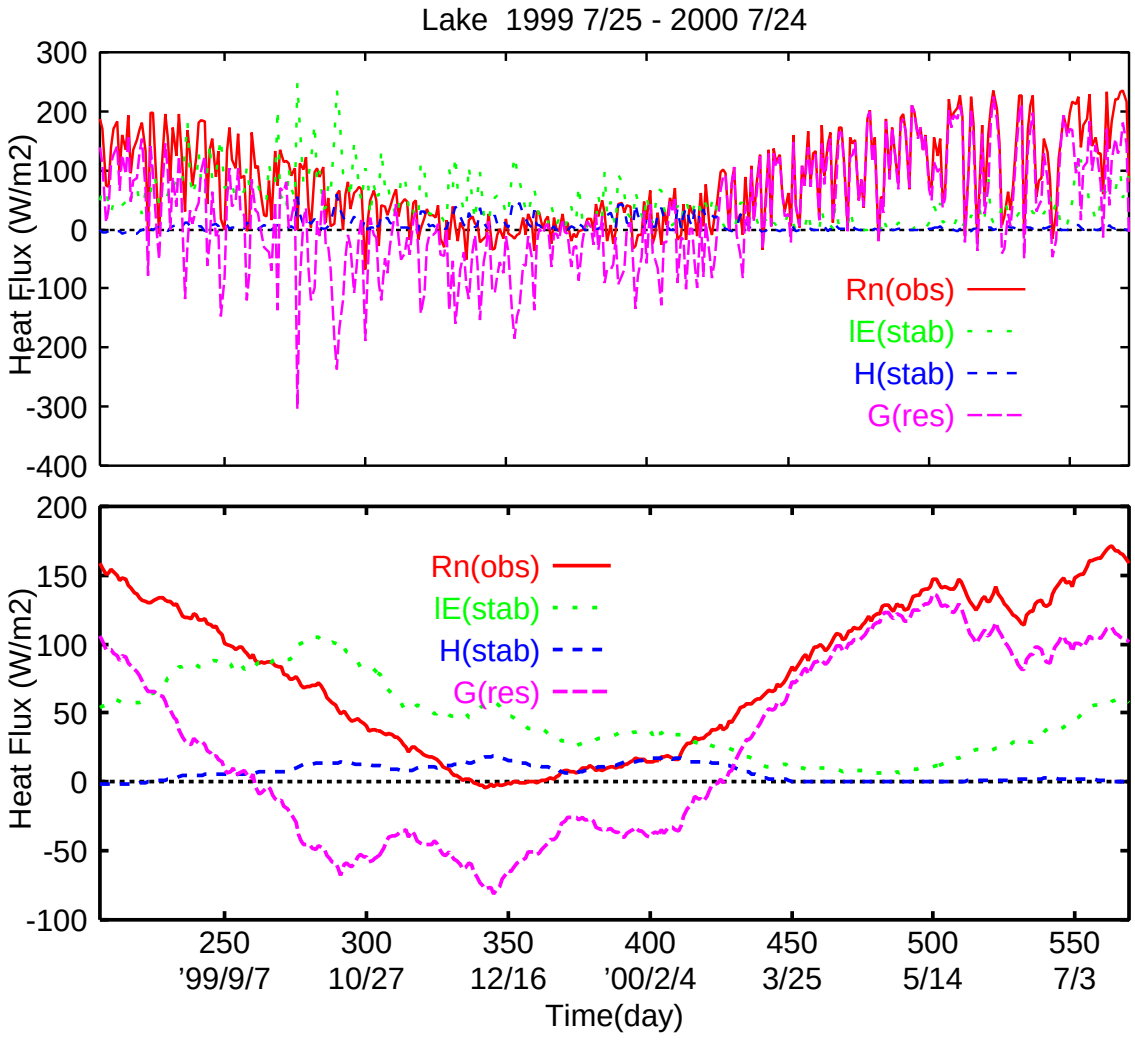

Figure 3.1: Seasonal variation of energy budget at the north part of the Lake Biwa (1999/7/25-2000/7/24). upper: daily average, lower: moving average of 15 days

3.2 Albedo and radiation budget

Figure 3.2 shows the seasonal variation of lake surface albedo from 25th July in 1999 to 24th July in 2000 by moving average of 15 days. Albedo becomes large in winter season and small in summer season. This is deeply related to the change in the solar zenith angle. **Figure 3.3** shows the relationship between the albedo (α) and cosine of zenith angle of incident solar radiation (μ). In this figure, data are selected according to the following criteria to see this dependency clearly.

$$S^{\downarrow} \geq 0.75 \times S_{top} \qquad S^{\downarrow} \geq 50 \quad (\mathrm{Wm}^{-2}) \qquad \mu \geq 0.1$$

where

$S^{\downarrow}$ = downward short-wave radiation observed at the surface
S_{top} = downward short-wave radiation at the top of atmosphere (theoretical value)

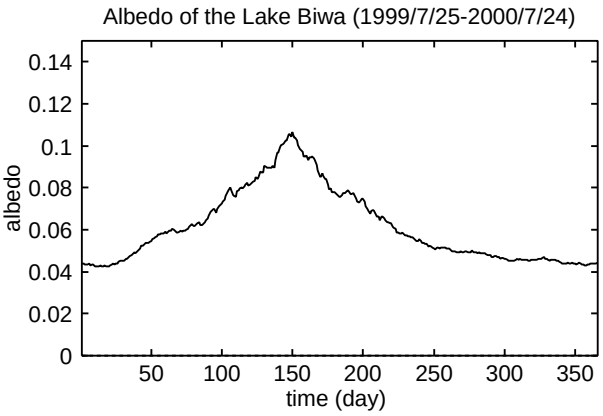

Figure 3.2: Albedo of the Lake Biwa (moving average of 15 days, 1999/7/25-2000/7/24)

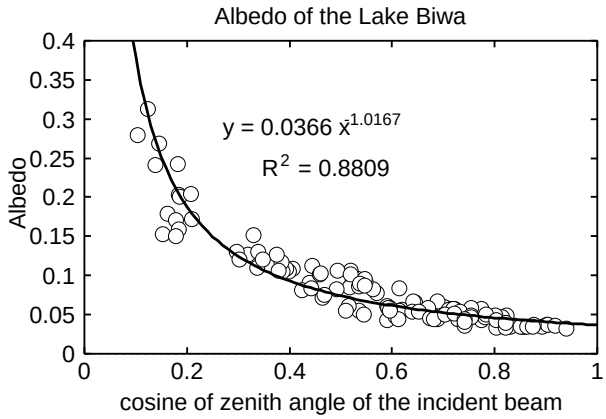

Figure 3.3: Dependency of albedo (α) on cosine of zenith angle of incident beam (μ)

When the sky is overcast or partly clouded, the propotion of direct beam radiation component becomes smaller than that of diffuse component. In that case, albedo shows the weakly dependency on the solar zenith angle. Anyway, the reflectance of water surface has strong dependency on μ for direct beam component. In the SiBUC model, following Goudriaan (1971), downward short-wave radiation is divided into four components (F_{vb} (visible-beam), F_{vd} (visible-diffuse), F_{nb} (near-infrared-beam), and F_{nd} (near-infrared-diffuse)) in the subroutine **goudriaan** (see **Appendix ??**) by the need of vegetation model (SiB). Then, we can treat direct beam component and diffuse component separately. The radiation budget for the water surface can be written as follows.

$$\alpha_b = a\mu^b \tag{3.1}$$

$$Rn_{wb} = (F_{vb} + F_{nb})(1 - \alpha_b) + (F_{vd} + F_{nd})(1 - \alpha_d) + F_{td} - \varepsilon_w \sigma T_{wb}^4 \tag{3.2}$$

Where, α_b and α_d are reflectance for direct beam component and diffuse component respectively. Unfortunately, direct beam component and diffuse component was not observed separately, we couldn't fix the relationship of **eq.(3.1)** directly. Actually, it is impossible to measure the propotion of reflected direct beam and reflected diffuse radiation. Therefore, the α_b and α_d are assumed to be equal, and the parameters in the relationship between reflectance and μ (**eq.(3.3)**) are decided through the the comparison of simulated and observed values (see **Section ??**).

$$\alpha_b = \alpha_d = \alpha_1 \mu^{\alpha_2} \tag{3.3}$$

3.3 Turbulent transfer and surface fluxes

Turbulent transfer process is very simple for the case of water body. Basically, the profile of wind, air temperature, and vapor pressure is expressed by log-linear law when atmosphere is in neutral condition. According to the Monin-Obukov similarity, aerodynamic resistance is calculated considering atmospheric stability.
Following Kondo(???), roughness is expressed by a function of friction velocity (**eq.(3.4)**). Friction velocity is a function of atmospheric stability. Stability is defined as a function of friction velocity and surface flux (**eq.(3.7)**). And the surface flux itself is a function of stability. Therefore, these values are determined through iteration procedure from a initial guess.

- **initial guess**
  $u_* = 0.001$ (m s^{-1}), neutral condition (ζ =0)

- **roughness and friction velocity (1st)**

$$\begin{aligned} u_{*c} &= 100 \times u_* \\ z_{0c} &= a \times u_{*c}^b \qquad (3.4) \\ z_0 &= 0.01 \times z_{0c} \\ u_* &= \kappa u_m / \ln(z_m/z_0) \qquad (3.5) \end{aligned}$$

when $u_{*c} \leq 6.89(cm)$
a = 1.69×10^{-2} b = -1.0
when $u_{*c} > 6.89(cm)$
a = 1.65×10^{-4} b = 1.4

Where, z_{0c} and u_{*c} are expressed in a unit of (cm), and z_0 and u_* are in (m).

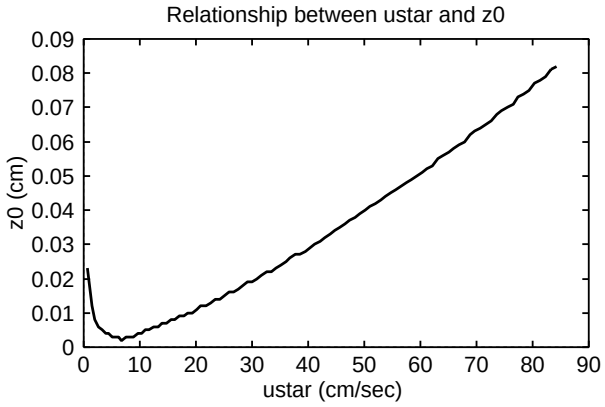

Figure 3.4: Relationship between friction velocity and roughness

- **stability (1st)**

$$H = \rho C_p(T_{wb} - T_m)\kappa u_* / \ln(z_m/z_{0h}), \quad E = \rho C_p(q_{wb} - q_m)\kappa u_* / \ln(z_m/z_{0h}) \qquad (3.6)$$
$$L = -\rho C_p T_m u_*^3/(\kappa g H_v), \quad H_v = H + 0.61(1 + 0.61 q_m) T_m C_p E \qquad (3.7)$$
$$\zeta = z_m/L, \qquad \zeta_0 = z_0/L \qquad (3.8)$$

In general, roughness for temperature and humidity are larger than that for momentum in the case of water surface. In this model, these are assumed to be equal to $z_{0h}(= 3z_0)$.

- **integrated universal function**

when $\zeta < 0$

$$\Psi_M = \ln\left(\frac{z_m}{z_0}\right) + \ln\frac{(x_0^2+1)(x_0+1)^2}{(x^2+1)(x+1)^2} + 2(\tan^{-1}x - \tan^{-1}x_0) \qquad (3.9)$$
$$\Psi_H = \ln\left(\frac{z_m}{z_{0h}}\right) + 2\ln\left(\frac{y_0+1}{y+1}\right) \qquad (3.10)$$
$$x = (1-16\zeta)^{1/4}, \; x_0 = (1-16\zeta_0)^{1/4}, \; y = (1-16\zeta)^{1/2}, \; y_0 = (1-16\zeta_0)^{1/2} \qquad (3.11)$$

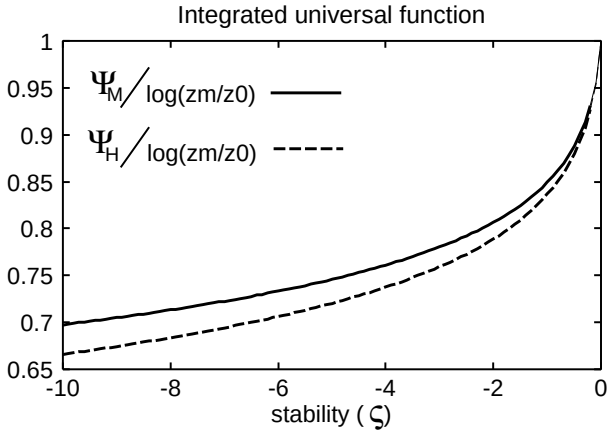

Figure 3.5: Relationship between stability and universal function (unstable)

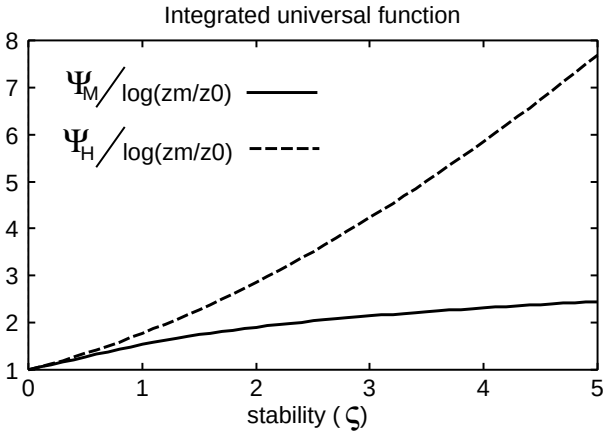

Figure 3.6: Relationship between stability and universal function (stable)

when $\zeta \geq 0$

$$\Psi_M = \ln\left(\frac{z_m}{z_0}\right) + \frac{7}{3}\ln\frac{1+3\zeta+10\zeta^3}{1+3\zeta_0+10\zeta_0^3} \tag{3.12}$$

$$\Psi_H = \ln\left(\frac{z_m}{z_{0h}}\right) + 400\ln\frac{1+7/400\zeta+0.005\zeta^2}{1+7/400\zeta_0+0.005\zeta_0^2} \tag{3.13}$$

- **friction velocity and stability (2nd)**

$$\begin{aligned} u_{*,2} &= \frac{\kappa u_m}{\Psi_M} \\ H &= \rho C_p(T_{wb}-T_m)\kappa u_{*,2}/\Psi_H, \quad E = \rho C_p(q_{wb}-q_m)\kappa u_{*,2}/\Psi_H \\ L &= -\rho C_p T_m u_{*,2}^3/(\kappa g H_v), \quad H_v = H + 0.61(1+0.61q_m)T_m C_p E \\ \zeta_2 &= z_m/L \end{aligned} \tag{3.14}$$

- **convergence condition**

$$|\zeta - \zeta_2| < 0.01 \qquad |(u_* - u_{*,2})/u_{*,2}| < 0.01$$

Above equation set is calculated iteratively until the convergence condition is obtained. Finally, momentum flux (τ_{wb}) and aerodynamic resistance between water surface and reference height (r_{aw}) are calculated from the result of friction velocity and integrated universal function.

$$\tau_{wb} = \rho u_*^2 \tag{3.15}$$

$$r_{aw} = \frac{\Psi_H}{\kappa u_*} = \frac{\Psi_M \Psi_H}{\kappa^2 u_m} \tag{3.16}$$

In the case of water body, sensible heat and latent heat fluxes come only from water surface. Although surface fluxes have already been calculated in the above iteration process, these fluxes are written in a resistance formulation. Note that these fluxes and net radiation (**eq.(3.2)**) are dependent on T_{wb} only.

$$H_{wb} = \rho C_p \frac{T_{wb} - T_m}{r_{aw}} = A(T_{wb} - T_m) \tag{3.17}$$

$$\lambda E_{wb} = \frac{\rho C_p}{\gamma} \frac{e_*(T_{wb}) - e_m}{r_{aw}} = D[e_*(T_{wb}) - e_m] \tag{3.18}$$

3.4 Prognostic variables and their governing equations

Water body model is expressed by force-restore model, and prognostic physycal-state variables are only two temperatures. One is water surface skin temperature (T_{wb}), another one is deep water temperature (T_{dw}), which is defined as daily mean value of T_{wb}. T_{wb} shows diurnal cycle, and T_{dw} shows seasonal cycle.
Most of the short-wave radiation absorbed by water body penetrate inside, and only little part of it are absorbed and used by surface skin layer. Then, amplitude of diurnal variation of water surface temperature is much smaller than those of other surfaces. While all long-wave radiation can be exchanged at water surface.
Absorbed short-wave energy is stored and used seasonally. Water body absorbs much energy in the spring and summer season, and this energy is released as latent heat (evaporation) in the autumn and winter season.
Then, the governing equations of temperatures in the water body are slightly different from those in the green area. In this model, we introduce a parameter β. It is defined as the propotion of short-wave radiative energy which are absorbed by water body and penetrate into deep layer. In the prognostic equation of surface temperature (**eq. (3.19)**), this propotion of absorbed short-wave energy is subtracted from net radiation (Rn_{wb}).
The governing equations of temperatures are expressed as follows.

$$C_{wb} \frac{\partial T_{wb}}{\partial t} = Rn_{wb} - \beta F_{s,wb} - H_{wb} - \lambda E_{wb} - \omega C_{wb}(T_{wb} - T_{dw}) \tag{3.19}$$

$$C_{dw} \frac{\partial T_{dw}}{\partial t} = Rn_{wb} - H_{wb} - \lambda E_{wb} \tag{3.20}$$

In addition to thermal properties such as specific heat (c_w) and thermal conductivity (k_w), four parameters are prepared to reproduce the energy and radiation budget characteristics properly.

- effective depth (Z_s)
- short-wave radiation penetration factor (β)
- minimum albedo (α_1)
- factor of albedo and μ relationship (α_2)

The role and performance of these parameters will be discussed in **Section ??**.
The amplitude and phase of seasonal cycle of temperature are highly dependent upon the depth of water body. To take account for the effect of water depth, effective depth (Z_s) is introduced in the calculation of effective heat capacity (**eq. (3.21)**) Z_s does not mean the actual depth of water body. If we look at **eq. (3.22)**, Z_s should be equal to or less than $1/\sqrt{365}$ of average water depth.

$$C_{wb} = c_w Z_s + \sqrt{k_w c_w / 2\omega} \tag{3.21}$$

$$C_{dw} = \sqrt{365} C_{wb} \tag{3.22}$$

3.5 Numerical solution of prognostic equations

The energy fluxes are explicit functions of atmospheric boundary conditions, prognostic variable, and aerodynamic resistance. Prognostic equations are solved by an implicit backward method using partial derivatives of each term.
First, considering the energy fluxes in prognostic equations are functions of temperature, partial derivatives are calculated in subroutine **partial**. Then, prognostic equations are expressed in explicit backward-differencing form and a set of linear simultaneous equations regarding the changes in temperatures over a time step (Δt) are obtained.
Not only energy fluxes but also heat exchange term (restoring term) has dependency on temperatures. Now prognostic equations can be written in discrete-time form.

$$\begin{aligned} C_{wb}\frac{\Delta T_{wb}}{\Delta t} &= Rn_{wb} - \beta F_{s,wb} - H_{wb} - \lambda E_{wb} - \omega C_{wb}(T_{wb} - T_{dw}) \\ &\quad + \frac{\partial Rn_{wb}}{\partial T_{wb}}\Delta T_{wb} - \frac{\partial H_{wb}}{\partial T_{wb}}\Delta T_{wb} - \frac{\partial \lambda E_{wb}}{\partial T_{wb}}\Delta T_{wb} - \omega C_{wb}(\Delta T_{wb} - \Delta T_{dw}) \quad (3.23) \\ C_{dw}\frac{\Delta T_{dw}}{\Delta t} &= Rn_{wb} - H_{wb} - \lambda E_{wb} + \frac{\partial Rn_{wb}}{\partial T_{wb}}\Delta T_{wb} - \frac{\partial H_{wb}}{\partial T_{wb}}\Delta T_{wb} - \frac{\partial \lambda E_{wb}}{\partial T_{wb}}\Delta T_{wb} \quad (3.24) \end{aligned}$$

If it is written in matrix form,

$$KX = Y \qquad \longrightarrow \qquad X = K^{-1}Y$$

$$K = \begin{bmatrix} \frac{C_{wb}}{\Delta t} - \frac{\partial Rn_{wb}}{\partial T_{wb}} + \frac{\partial H_{wb}}{\partial T_{wb}} + \frac{\partial \lambda E_{wb}}{\partial T_{wb}} + \omega C_{wb} & \omega C_{wb} \\ -\frac{\partial Rn_{wb}}{\partial T_{wb}} + \frac{\partial H_{wb}}{\partial T_{wb}} + \frac{\partial \lambda E_{wb}}{\partial T_{wb}} & \frac{C_{dw}}{\Delta t} \end{bmatrix} \qquad X = \begin{bmatrix} \Delta T_{wb} \\ \Delta T_{dw} \end{bmatrix}$$

$$Y = \begin{bmatrix} Rn_{wb} - \beta F_{s,wb} - H_{wb} - \lambda E_{wb} - \omega C_{wb}(T_{wb} - T_{dw}) \\ Rn_{wb} - H_{wb} - \lambda E_{wb} \end{bmatrix}$$

Above equations can be solved in terms of temperature changes ($\Delta T_{wb}, \Delta T_{dw}$). Each temperatures are updated to the value at time $t_0 + \Delta t$ by adding temperature changes to the initial value at time t_0. Furthermore, energy fluxes are modified to show the values averaged over a time step (between time t_0 and time $t_0 + \Delta t$).

$$\begin{aligned} Rn'_{wb} &= Rn_{wb} + \frac{1}{2}\frac{\partial Rn_{wb}}{\partial T_{wb}}\Delta T_{wb} \quad (3.25) \\ H'_{wb} &= H_{wb} + \frac{1}{2}\frac{\partial H_{wb}}{\partial T_{wb}}\Delta T_{wb} \quad (3.26) \\ \lambda E'_{wb} &= \lambda E_{wb} + \frac{1}{2}\frac{\partial \lambda E_{wb}}{\partial T_{wb}}\Delta T_{wb} \quad (3.27) \end{aligned}$$

According to **eq.(3.2), (3.17), (3.18)**, partial derivatives of energy fluxes are expressed as follows.

$$\begin{aligned} \frac{\partial Rn_{wb}}{\partial T_{wb}} &= -4\sigma\varepsilon_w T_{wb}^3 \quad (3.28) \\ \frac{\partial H_{wb}}{\partial T_{wb}} &= \frac{\rho_a C_p}{r_{aw}} \quad (3.29) \\ \frac{\partial \lambda E_{wb}}{\partial T_{wb}} &= \frac{\rho C_p}{\gamma}\frac{e'_*(T_{wb})}{r_{aw}} \quad (3.30) \end{aligned}$$

Chapter 4

Green area model

In this chapter, green area model to be used as sub-model of SiBUC is described. Vegetation scheme is based largely on the SiB model (Sellers et al.,1986). Some modification (simplification) from original SiB was done. Variables and parameters used in the green area model are listed in **Table 4.1** and **4.2**. Physical constants are listed in **Table A.1** in **Appendix A**. Definition of forcing variables and prognostic variables can be found in **Table 1.1**.

Table 4.1: List of variables used in the green area model

Symbol	Definition	Units
Rn_c, Rn_g	absorbed net radiation absorbed	W m^{-2}
H_c, H_g	sensible heat flux	W m^{-2}
$\lambda E_c, \lambda E_g$	latent heat flux	W m^{-2}
C_c, C_g, C_d	effective heat capacity	J $m^{-2}K^{-1}$
k_s	soil thermal conductivity	$Wm^{-1}K^{-1}$
c_s	soil heat capacity	J $m^{-3}K^{-1}$
E_s	direct evaporation of water from the surface soil layer	kg $m^{-2}s^{-1}$
$E_{dc,1}, E_{dc,2}$	abstraction of soil moisture by transpiration	kg $m^{-2}s^{-1}$
E_{wc}, E_{wg}	rate of evaporation of water from wet portions	kg $m^{-2}s^{-1}$
P_c, P_g	rate of precipitation interception	m s^{-1}
D_c, D_g	water drainage rate	m s^{-1}
P_1	infiltration of precipitation into the upper soil layer	m s^{-1}
$Q_{1,2}, Q_{2,3}$	flow between soil layer	m s^{-1}
Q_3	gravitational drainage from recharge layer	m s^{-1}
K_i	hydraulic conductivity of ith layer	m s^{-1}
ψ_i	soil moisture potential of ith layer	m
ψ_l	leaf water potential	m
ψ_r	soil moisture potential in root zone	m
r_b	bulk canopy boundary layer resistance	s m^{-1}
r_d	aerodynamic resistance between ground and canopy air space	s m^{-1}
r_a	aerodynamic resistance between canopy air space and reference height	s m^{-1}
r_c	bulk canopy resistance	s m^{-1}
r_{surf}	bare soil surface resistance	s m^{-1}

The subscript c refers to the canopy, g to the ground, and d to the deep soil.

Table 4.2: List of parameters used in the green area model

Symbol	Definition	Unit
	Time-invariant vegetation parameters	
	morphological properties	
z_2	height of canopy top	m
z_1	height of canopy bottom	m
z_c	inflection height for leaf-area density	m
z_s	ground roughness length (0.05)	m
V_c	canopy cover fraction	—
χ_L	Ross-Goudriaan leaf-angle distribution factor	—
G_1, G_4	momentum transfer coefficient parameters (1.449, 11.785)	—
l_w, l_l	leaf dimension (width, length)	m
D_1	depth of surface soil layer (0.02)	m
D_r	root depth ($D_1 + D_2$)	m
D_T	total soil depth ($D_1 + D_2 + D_3$)	
D_d	root length density	m m^{-3}
$\oslash_s$	mean topographic slope (0.176)	radians
	optical properties	
α_V	leaf reflectance for visible	—
α_N	leaf reflectance for near infra-red	—
δ_V	leaf transmittance for visible	—
δ_N	leaf transmittance for near infra-red	—
$\alpha_{s,V}$	soil reflectance for visible	—
$\alpha_{s,N}$	soil reflectance for near infra-red	—
	physical properties	
C_l	drag coefficient of a canopy leaf	—
C_s	heat/vapor transfer coefficient of a canopy leaf	—
	physiological properties	
a_2, b_2, c_2	light dependent stomatal response parameters	
T_l, T_h, T_o	lowest, highest, and optimum temperatures for stomatal functioning	K
h_5	parameter governing stomatal response to the vapor pressure	mb^{-1}
ψ_{c1}	leaf water potential at which stomata start to close	m
ψ_{c2}	leaf water potential at which stomata are completely closed	m
r_{plant}	resistance imposed by plant vascular system (2.5×10^8)	s
R	root resistance per unit area (4.0×10^12)	s m^{-1}
	Time-varying vegetation parameters	
L_T	total leaf area index	m^{2}m^{-2}
N	canopy greenness fraction	—
	Soil physical properties	
ψ_s	soil water potential at saturation	m
K_s	soil hydraulic conductivity at saturation	ms^{-1}
B	soil wetness parameter	—
θ_s	soil water content at saturation (porosity)	m^{3}m^{-3}

4.1 Brief description of SiB model

The Simple Biosphere model (SiB) was designed for use within GCMs. As for a full description of the philosophy, design and requirements of the model, please refer to Sellers et al.(1986).

4.1.1 Model philosophy

In designing the SiB model, the philosophy was to model the vegetation itself and thereby calculate the radiation, momentum, heat and mass transfer properties of the surface in a consistent way. The morphological and physiological characteristics of the vegetation community at a grid point are used to derive coefficients and resistances which govern the fluxes between the surface and the atmosphere. All of these fluxes depend upon the state of the vegetated surface and the atmospheric boundary conditions.
The SiB model calculates following physical processes.

1. the reflection, transmission, absorption and emission of direct and diffuse radiation in the visible, near infrared and thermal wavelength intervals (radiative transfer)

2. the interception of rainfall and its evaporation from the leaf surfaces (interception loss)

3. the infiltration, drainage, and storage of the residual rainfall in the soil (soil moisture)

4. the control by the photosynthetically active radiation (PAR) and the soil moisture potential over the stomatal functioning (canopy resistance)

5. transfer of the soil moisture to the atmosphere through the root-stem-leaf system of the vegetation (transpiration)

6. the aerodynamic transfer of water vapor, sensible heat and momentum from the vegetation and soil to a reference level within the atmospheric boundary layer (turbulent flux)

4.1.2 Structure of the SiB

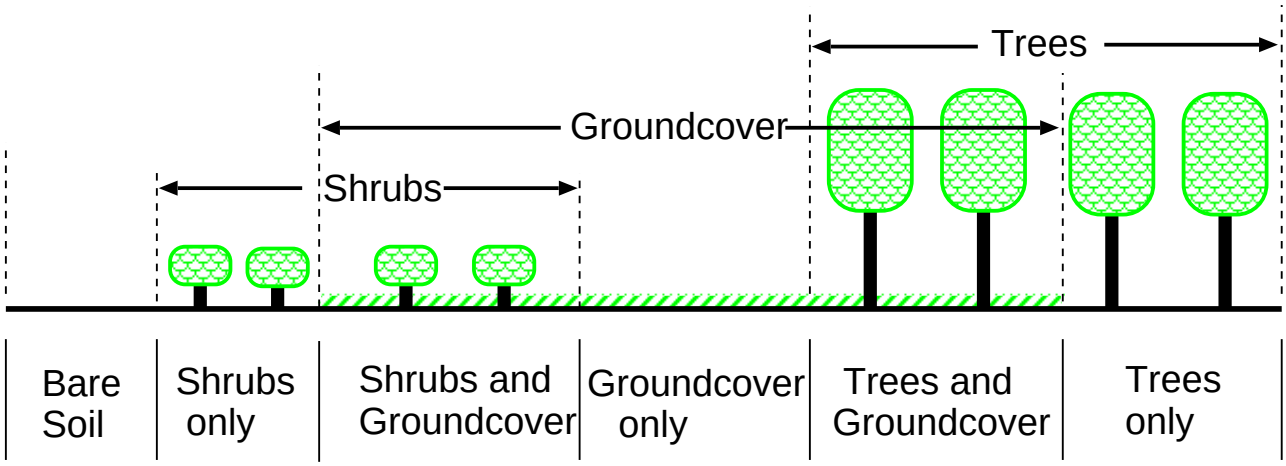

Figure 4.1: Vegetation morphology as represented in the Simple Biosphere (SiB). (Reproduced from *Sellers et al.,1986***)**

In SiB, the world's vegetation is divided into two morphological groups : trees or shrubs which constitute the upper story or canopy vegetation, and the ground cover which consists of grasses and other herbaceous plants. Either, both or neigher of these vegetation covers may be present in a given grid area (see **Figure 4.1**). The upper story vegetation consists of perennial plants with persistent roots assigned to a fixed depth taken to be the bottom of the second soil layer. The ground cover is made up of annual plants and may have a time-varying root depth.
There is an upper, thin soil layer (soil layer 1), from which there can be a significant rate of wathdrawal of water by direct evaporation into the air when the pores of the soil are at or near saturation. Beneath the root zone (soil layer 2), there is an underlying recharge layer (soil layer 3) where the transfer of water is governed only by gravitational drainage and hydraulic diffusion. The parameters required for each vegetation type in SiB are listed in Table 1 of Sellers et al.(1986). Values for many of the parameters are given in Dorman and Sellers (1989).

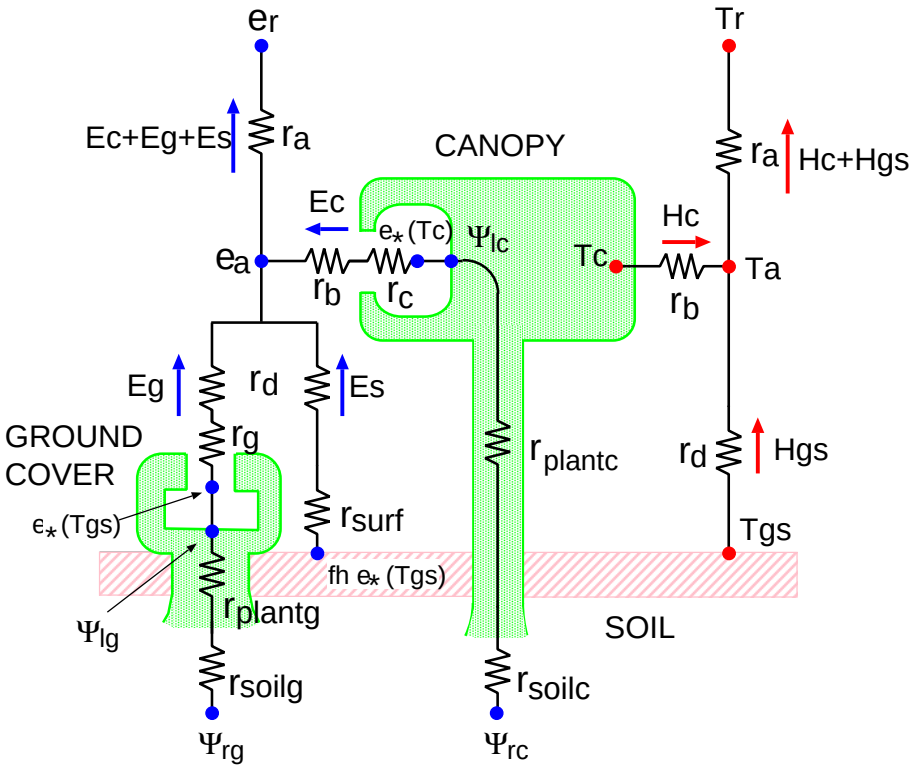

Figure 4.2: Framework of the SiB. The transfer pathways for latent and sensible heat fluxes are shown on the left- and right-hand sides of the diagram, respectively.(Reproduced from *Sellers et al.,1986*; see this reference for symbol definitions.)

4.1.3 Atmospheric boundary conditions for SiB

The upper boundary conditions for SiB are as follows :

- Air temperature, vapor pressure and wind speed of the lowest model layer (reference height), — T_m, e_m, u_m

- The solar zenith angle, — μ

- Five components of the incident radiation, — $F(0)$
  $F_{v,b(0)}$ Visible or PAR ($< 0.72\mu m$) direct beam radiation
  $F_{v,d(0)}$ Visible or PAR ($< 0.72\mu m$) diffuse radiation
  $F_{n,b(0)}$ Near infrared ($0.72 - 4.0\mu m$) direct beam radiation
  $F_{n,d(0)}$ Near infrared ($0.72 - 4.0\mu m$) diffuse radiation
  $F_{t,d(0)}$ Thermal infrared ($8.0 - 12.0\mu m$) difuse radiation

- Large scale and convective precipitation rates, — P_L, P_C

The reference height (z_m) is selected within the atmospheric boundary layer (usually the upper side of surface layer, 30 - 50(m)).
μ can be calculated from the location (latitude, longitude), date, and time. The propotions of the various spectral and angular fractions of short-wave incoming radiation are estimated from the scheme of Goudriaan (1977), since they are not usually provided by atmospheric models.
If P_L and P_C are not available, total precipitation ($P_L + P_C$) is used as input value.

4.1.4 Prognostic physical-state variables of SiB

The SiB has eight prognostic physical-state variables.

- Three temperatures
  T_c (canopy), T_{gs} (ground cover and soil surface), T_d (deep soil)

- two interception water stores
  M_c (canopy), M_g (ground cover)

- three soil moisture stores
  W_1 (surface layer), W_2 (root zone), W_3 (recharge layer)

4.2 Structure of the green area model

SiB had two vegetation layers for canopy and ground-cover. In the green area model, vegetation layer is reduced to one as SSiB (Xue et al., 1991) and SiB2 (Sellers et al, 1996) does. It was necessary to reduce these to one layer in SiB2 to incorporate the iterative photosynthesis-conductance model and to make use of satellite data to describe surface parameters. This simplification reduces the realism of SiB2 in areas that have two-story vegetation covers, such as savannah where C_3 trees overlie C_4 grasslands.
The green area model, presented here, also uses satellite data to calculate time-varying vegetation parameters such as leaf area index (see **Chaper ??**). Therefore, both "canopy" and "ground cover" in SiB are called "canopy" and treated together in this model. The schematic image of surface elements of the green area model is shown in **Figure 4.3**.
The root and soil models of the green area model are much the same as in SiB. The roots are assumed to access the soil moisture from the second layer of a three-layer soil model, while the third layer acts as a source for hydrological baseflow and upward recharge of the root zone. The uppermost thin soil layer can act as a significant source of direct evaporation when the soil surface is wet.
Each vegetation type is assigned a set of time-invariant parameters (see **Table 4.2**). These include (i) morphological parameters; (ii) optical properties; and (iii) physiological properties.

These properties are treated as constants for each vegetation type (**Table 4.3**). Time-varying quantities such as leaf area index may be combined with these parameters to produce further quantities. In SiB, soil properties were assigned to each vegetation type in much the same way as the time-invariant vegetation properties. However, soil properties exhibit regional variations that can be independent of vegetation type, and vice versa. In the green area model, same as SiB2, Food and Agriculture Organization (FAO) global soil-type map is used to assign a soil type to each grid element (see **Chapter ??**).

Table 4.3: Vegetation classification schemes used in SiB2 and green area model

Type	Name
1	Broadleaf-evergreen trees
2	Broadleaf-deciduous trees
3	Broadleaf and needleleaf trees
4	Needleleaf-evergreen trees
5	Needleleaf-deciduous trees
6	Short vegetation/C4 grassland
7	Broadleaf shrubs with bare soil
8	Dwarf trees and shrubs
9	Agriculture/C3 grassland

If there is a need to identify two vegetation types within one grid area, we can further divide the green area into two (mosaic of two tiles), that is :

$$V_{ga} = V_{ga,1} + V_{ga,2} \tag{4.1}$$

where $V_{ga,1}$ and $V_{ga,2}$ are the fractional areas of "type 1" and "type 2" vegetation, respectively. Since the main concern of SiBUC is a heterogeneity between natural vegetation and urbanized area and water body, one green area (one tile for green area) is a default setting of the green area model.

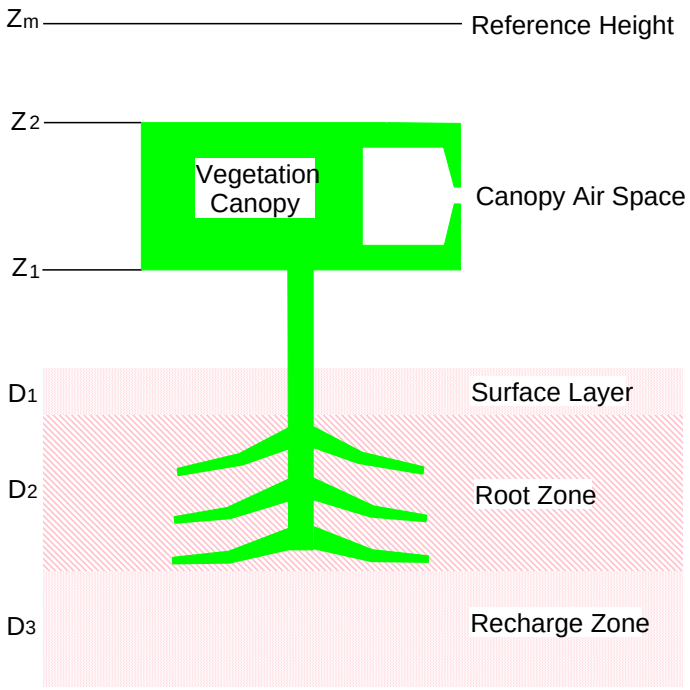

Figure 4.3: Structure of the green area model. (Reproduced from *Sellers et al.,1996***)**

4.3 Prognostic equations of the green area model

The prognostic physical-state variables of the green area model is basically same as SiB. The difference in the definition of prognostic variables between SiB and our model is the treatment of ground cover.

- Three temperatures
  T_c (vegetation canopy), T_g (ground), T_d (deep soil)
- two interception water stores
  M_c (canopy), M_g (ground)
- three soil moisture stores
  W_1 (surface layer), W_2 (root zone), W_3 (recharge layer)

4.3.1 Governing equations for temperatures

In case of the green area model, two surface temperatures (T_c, T_g) are predicted to calculate the surface fluxes. Heat transport in the soil is described by the force-restore model of Deardorff (1977). The force-restore approximation relies on the analytical solution of the heat conduction equation under periodic forcing, which is used to parameterize the almost periodic daily ground heat flux. In this way, a very simple and efficient but reasonably accurate description of the temperature dynamics can be achieved. Since the the heat conduction term through the step of vegetation is negligible[1], prognostic equation for T_c does not have restoring term. Therefore, the governing equations for the three temperatures are expressed as follows.

$$C_c \frac{\partial T_c}{\partial t} = Rn_c - H_c - \lambda E_c \tag{4.2}$$

$$C_g \frac{\partial T_g}{\partial t} = Rn_g - H_g - \lambda E_g - \omega C_g (T_g - T_d) \tag{4.3}$$

$$C_d \frac{\partial T_d}{\partial t} = Rn_g - H_g - \lambda E_g \tag{4.4}$$

The heat capacity of the diurnally responsive upper soil (C_g) is defined after the work of Camilo and Schmugge (1981), who formulated expressions for soil thermal conductivity (k_s) and specific heat (c_s) as function of porosity and soil moisture content.

$$C_c = 0.0001\ L_T\ C_w\ \rho_w \tag{4.5}$$

$$C_g = \left(\frac{c_s k_s}{2\omega}\right)^{1/2} \tag{4.6}$$

$$C_d = \sqrt{365} C_g \tag{4.7}$$

$$k_s = 0.4186 \frac{1.5(1-\theta_s) + 1.3\theta_s W_1}{0.75 + 0.65\theta_s - 0.4\theta_s W_1} \tag{4.8}$$

$$c_s = [0.5(1-\theta_s) + \theta_s W_1] C_w \rho_w \tag{4.9}$$

In **eq.(4.5)**, the thickness of canopy leaves are assumed to be 1 (mm). As for **eq.(4.7)**, heat capacity is propotional to a square root of cycle. T_d is defined as mean value of T_g over one day, and T_d is expected to have seasonal cycle (one year). The effective heat capacity is impotant for reproducing the amplitude and phase of diurnal cycle.

[1]Radiative transfer is important for the exchange of energy between canopy and ground surface.

4.3.2 Governing equations for intercepted water

The governing equations for the two interception water stores are expressed in the same formula.

$$\frac{\partial M_c}{\partial t} = P_c - D_c - \frac{E_{wc}}{\rho_w} \tag{4.10}$$

$$\frac{\partial M_g}{\partial t} = P_g - D_g - \frac{E_{wg}}{\rho_w} \tag{4.11}$$

$$\tag{4.12}$$

This is simple water budget equation for water store. In the calculation of water store (M_c, M_g), evaporation (E_{wc}, E_{wg}) is modified if a negative value of $M_c or M_g$ is produced.

The interception and evaporation of precipitation stored on the canopy and the ground is modeled simply. **Figure 4.4** shows the schematic image of precipitation interception and water budget in the green area model. The maximum values for water store (S_c and S_g) are set to each story. If the water store (M_c or M_g) exceeds the maximum value, the drainage (D_c or D_g) occurs.
First, the interception of the rainfall by the canopy is determined by an adaptation of the expression describing the exponential attenuation of radiation when the flux is vertical and the leaves are black (no reflection). The rate of inflow (interception) and outflow (drainage) for the canopy are given as follows.

$$P_c = PV_c(1 - e^{-L_T K_c}) \tag{4.13}$$

$$\begin{aligned} D_c &= 0 \quad \text{when} M_c < S_c \\ &= P_c \quad \text{when} M_c = S_c \end{aligned} \tag{4.14}$$

The water actually captured by the canopy is $P_c - D_c$, Therefore, the effective precipitation for the ground surface is given by

$$P_0 = P - (P_c - D_c) \tag{4.15}$$

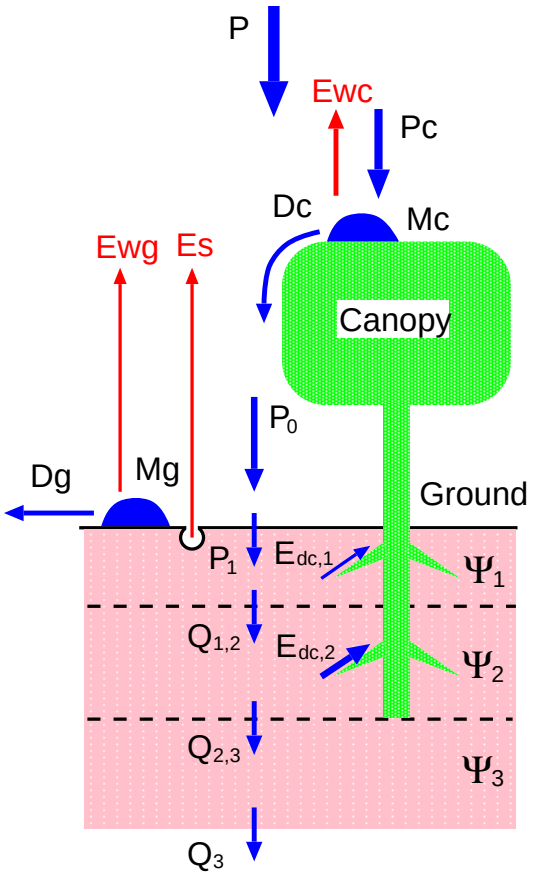

Figure 4.4: Schematic image of interception and water budget

Some of the effective precipitation can infiltrate into surface soil layer. When P_0 is stronger than the hydraulic conductivity at saturation (K_s), 'infiltration excess' runoff occures. And if the surface soil layer is saturated, 'saturation excess' runoff occures.

$$\begin{aligned} P_1 &= P_0 \quad \text{when} P_0 \leq K_s \ \ and \ \ W_1 < 1 \\ &= K_s \quad \text{when} P_0 > K_s \ \ and \ \ W_1 < 1 \\ &= 0 \quad \text{when} W_1 = 1 \end{aligned} \tag{4.16}$$

Now $P_0 - P_1$ becomes the inflow to the surface water store (M_g).

$$\begin{aligned} P_g &= P_0 - P_1 && (4.17) \\ D_g &= 0 \qquad \text{when} M_g < S_g \\ &= P_g \qquad \text{when} M_g = S_g && (4.18) \end{aligned}$$

Therefore, the total runoff from the green area (R_{ga}) is given by summing surface runoff (D_g) and baseflow (Q_3) expressed by **eq.(4.24)**.

$$R_{ga} = D_g + Q_3 \tag{4.19}$$

4.3.3 Governing equations for soil moisture stores

The governing equations for the three soil moistures is based on Richards' equation with forcing terms of evapotranspiration ($E_s, E_{dc,1}, E_{dc,2}$) and infiltration (P_1).

$$\begin{aligned} \frac{\partial W_1}{\partial t} &= \frac{1}{\theta_s D_1}\left[P_1 - Q_{1,2} - \frac{1}{\rho_w}(E_s + E_{dc,1})\right] \\ \frac{\partial W_2}{\partial t} &= \frac{1}{\theta_s D_2}\left[Q_{1,2} - Q_{2,3} - \frac{E_{dc,2}}{\rho_w}\right] \\ \frac{\partial W_3}{\partial t} &= \frac{1}{\theta_s D_3}\left[Q_{2,3} - Q_3\right] \end{aligned}$$

A three-layer isothermal model is used to calculate the hydraulic diffusion and gravitational drainage of water in the soil. The equation used to describe vertical exchanges between soil layers is expressed by Darcy's law.

$$Q_{i,i+1} = K\left[\frac{\partial \psi}{\partial z} + 1\right] = \overline{K}\left[\frac{2(\psi_i - \psi_{i+1})}{D_i + D_{i+1}} + 1\right] \quad (i = 1, 2) \tag{4.20}$$

$$\overline{K} = \frac{D_i K_i + D_{i+1} K_{i+1}}{D_i + D_{i+1}} \tag{4.21}$$

In **eq.(4.20)**, the term "1" accounts for gravitational drainage. When $Q_{i,i+1}$ is positive, flow is downward. As for the relationship between soil physical properties, Clapp and Hornberger (1978) is used.

$$\begin{aligned} K_i &= K_s W_i^{2B+3} && (4.22) \\ \psi_i &= \psi_s W_i^{-B} && (4.23) \end{aligned}$$

The flow out of the bottom of soil column to create base flow is determined by gravitational drainage only.

$$Q_3 = \sin \oslash_s \; K_s \; W_3^{2B+3} \tag{4.24}$$

Where $\oslash_s$ is defined as "mean topographic slope". However, is is almost meaningless if the grid size is larger than the size of actual slope of mountain.
The infiltration of liquid water (P_1) is assumed to be zero when the ground temperature (T_g) is below the freezing point of water.

4.4 Radiative transfer (two-stream approximation)

The two-stream approximation model (Dickinson, 1983) was extended by Sellers (1985) to describe the interception, reflection, transmission, and absorption of radiation by vegetation and soil. The radiation model used in the green area model is same as SiB2. Since there is only one vegetation layer, a single set of calculations for the canopy-soil system (one for each radiation component) is performed each time step. Following the solution of the two-stream approximation model for the canopy-ground system, the canopy reflectances, absorbances, and transmittances are specified and the radiation absorbed by the canopy and soil from each incident component is calculated. Reflected and emitted fluxes are used as lower boundary conditions for the atmospheric radiation submodel.
The original equations as specified by Dickinson (1983) are as follows.

$$-\overline{\mu}\frac{dI\uparrow}{dL} + [1-(1-\beta)(\alpha+\delta)]I\uparrow - (\alpha+\delta)\beta I\downarrow = (\alpha+\delta)\overline{\mu}K\beta_0 e^{-KL} \quad (4.25)$$

$$\overline{\mu}\frac{dI\downarrow}{dL} + [1-(1-\beta)(\alpha+\delta)]I\downarrow - (\alpha+\delta)\beta I\uparrow = (\alpha+\delta)\overline{\mu}K(1-\beta_0)e^{-KL} \quad (4.26)$$

where

$I\uparrow, I\downarrow$	=	upward and downward diffuse radiative fluxes (normalized by the incident flux)
μ	=	cosine of zenith angle of the incident beam
K	=	optical depth of the direct beam per unit leaf area = $G(\mu)/\mu$
$G(\mu)$	=	projected area of leaf elements in direction μ
$\overline{\mu}$	=	average inverse diffuse optical depth per unit leaf area
β, β_0	=	upscatter parameters for the diffuse and direct beams
L	=	cumulative leaf area index

The values of the parameters $K, G(\mu), \overline{\mu}$ are functions of canopy geometry, specifically the leaf angle distribution function. The values of the upscatter parameters β and β_0 are functions of both canopy geometric and optical properties.
In SiB2, specification of the leaf angle distribution is done by means of the χ_L function of Ross (1975), whereby the departure of leaf angles from a spherical distribution is characterized by a simple expression.

$$\chi_L = \int_0^{\pi/2} |1 - O(\theta)| \sin\theta d\theta \quad (4.27)$$

where

θ	:	the leaf inclination angle relative to a horizontal plane
$O(\theta)$	:	leaf-angle distribution function

- $\chi_L = 0$: spherically (random) distribution
- $\chi_L = 1$: horizontal leaves
- χ_L = -1 : vertical leaves

Goudriaan (1977) fitted a curve to datasets generated from **eq.(4.27)**, which provides reasonable estimates of the average leaf projection in any direction.

$$G(\mu) = \phi_1 + \phi_2\mu \tag{4.28}$$
$$\phi_1 = 0.5 - 0.633\chi_L - 0.33\chi_L^2 \tag{4.29}$$
$$\phi_2 = 0.877(1 - 2\phi_1) \tag{4.30}$$

Equation (4.28) may be used over the range $-0.4 < \chi_L < 0.6$. Field data have been analyzed to specify χ_L for different biomes. χ_L is also used to describe the aerodynamic resistances (see **Section 4.5**).

The two equations **(4.25)** and **(4.26)** are solved using the incident (above canopy) radiation flux and the upwelling diffuse flux refrected by the soil as upper and lower boundary conditions, respectively. The calculation is performed for each of the four solar radiation components with a different simplified calculations for the exchanges of thermal infrared radiation.

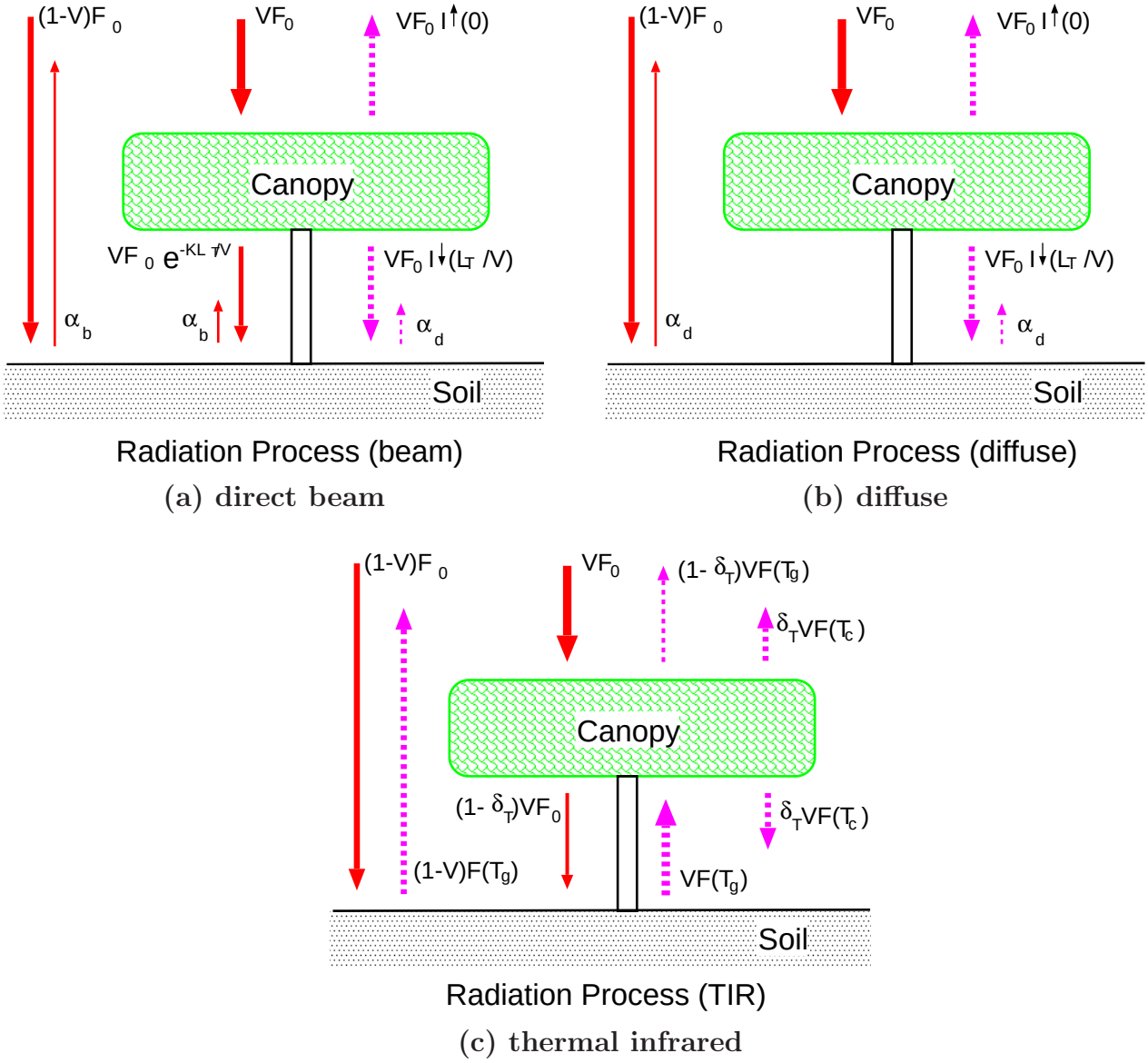

Figure 4.5: Schematic image of radiative transfer model

Figure 4.5 describes each term of radiation components for direct beam, diffuse and thermal-infrared radiation. The downward flux of diffuse radiation in the canopy $I \downarrow$ has three components.

- a component resulting from interception and rescattering of the direct beam radiation
- an exponentially extinguished downward flux resulting from downward scattering in the canopy
- an exponentially attenuated upwards flux resulting from upward scattering of radiation by canopy leaves and soil.

The upward diffuse flux ($I\uparrow$) also has similar components. $I\uparrow(0)$ can be used as the canopy-soil system hemispherical reflectance, while $I\downarrow(L_T/V) + e^{-KL_T/V}$ defines the spectral transmittance of the vegetation.

The direct beam solar radiation absorbed by the canopy ($F_{V/N,b(c)}$) and ground ($F_{V/N,b(g)}$) is given as follows.

$$F_{\Lambda,b(c)} = V\left[1 - I^{\uparrow}(0) - (1-\alpha_{\Lambda,b})e^{-KL_T/V_c} - (1-\alpha_{\Lambda,d})I^{\downarrow}(L_T/V_c)\right]F_{\Lambda,b(0)} \quad (4.31)$$

$$F_{\Lambda,b(g)} = \left[(1-V_c)(1-\alpha_{\Lambda,b}) + V_c\left((1-\alpha_{\Lambda,b})e^{-KL_T/V_c} + (1-\alpha_{\Lambda,d})I^{\downarrow}(L_T/V_c)\right)\right]F_{\Lambda,b(0)} \quad (4.32)$$

The diffuse solar radiation absorbed by the canopy ($F_{\Lambda,d(c)}$) and ground ($F_{\Lambda,d(g)}$) is given as follows.

$$F_{\Lambda,d(c)} = V_c\left[1 - I^{\uparrow}(0) - (1-\alpha_{\Lambda,d})I^{\downarrow}(L_T/V_c)\right]F_{\Lambda,d(0)} \quad (4.33)$$

$$F_{\Lambda,d(g)} = \left[(1-V_c)(1-\alpha_{\Lambda,d}) + V_c(1-\alpha_{\Lambda,d})I^{\downarrow}(L_T/V_c)\right]F_{\Lambda,d(0)} \quad (4.34)$$

The net absorbed thermal radiation fluxes are given by

$$F_{T,d(c)} = \delta_T V_c F_{T,d(0)} - 2\delta_T V_c \sigma T_c^4 + \delta_T V_c \sigma T_g^4 \quad (4.35)$$

$$F_{T,d(g)} = (1-\delta_T V_c)F_{T,d(0)} + \delta_T V_c \sigma T_c^4 - \sigma T_g^4 \quad (4.36)$$

$F_{\Lambda,\mu(0)}$	=	incident radiant solar energy of wavelength interbal Λ and direction μ (V = visible, N = near-infrared) and (d = diffuse, b = beam)	W m^{-2}
$F_{\Lambda,\mu(c)}$	=	amount of $F_{\Lambda,\mu(0)}$ absorbed by the canopy	W m^{-2}
$F_{\Lambda,\mu(g)}$	=	amount of $F_{\Lambda,\mu(0)}$ absorbed by the ground	W m^{-2}
$F_{T,d(0)}$	=	incident thermal infrared radiation (TIR)	W m^{-2}
$V\delta_T$	=	fraction of incident TIR absorbed by canopy	
δ_T	=	1 - $e^{-L_T/V_c\overline{\mu}}$	

In **eq.(4.35)** and **eq.(4.36)**, ground and canopy emissivities are assumed to approach unity. The net radiation fluxes for canopy and ground are given by the total of absorbed flux components.

$$Rn_c = \sum F_{\Lambda,\mu(c)} = F_{V,b(c)} + F_{N,b(c)} + F_{V,d(c)} + F_{N,d(c)} + F_{T,d(c)} \quad (4.37)$$

$$Rn_g = \sum F_{\Lambda,\mu(g)} = F_{V,b(g)} + F_{N,b(g)} + F_{V,d(g)} + F_{N,d(g)} + F_{T,d(g)} \quad (4.38)$$

4.5 Turbulent transfer and aerodynamic resistances

The aerodynamic resistance model of SiB (Sellers et al.,1986) described turbulent transfer processes above, within, and below a vegetation canopy of "constant leaf area density". This arrangement was found to give unrealistically large estimates of roughness length (z_0). Then, the scheme was modified to describe height-varying leaf area densities (Sellers et al.,1989). In this modified form, the first-order closure model provided much better descriptions of z_0, d_0, and the wind profile. This improved version of the turbulent transfer scheme is used in SiB2 (Sellers et al.,1996) and also adopted to the green area model.
Figure 4.5 shows the different turbulent transfer regimes considered in the first-order closure model.

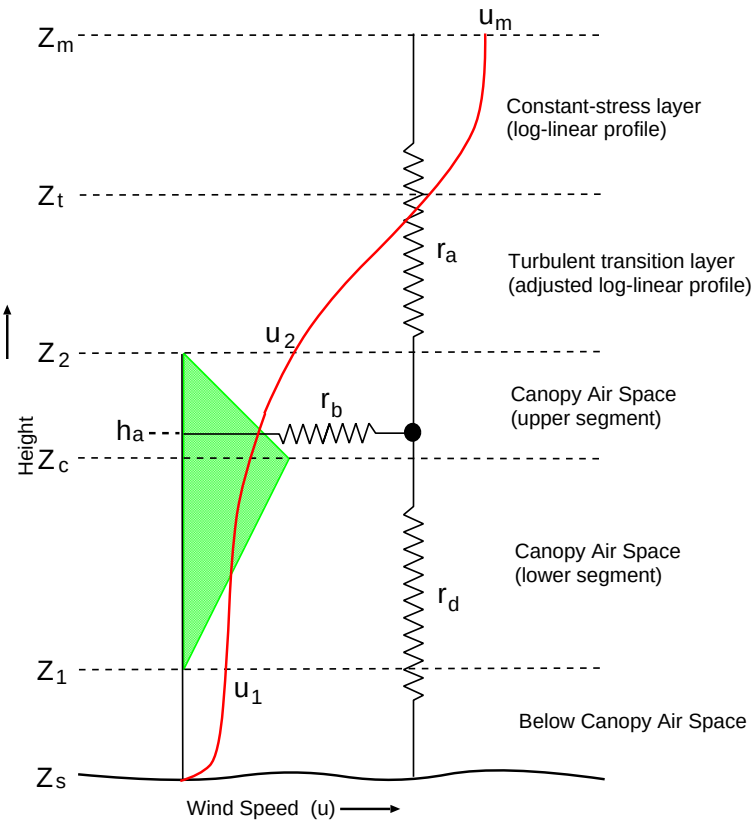

Figure 4.6: Turbulent transfer regimes considered in the first-order closure model. (Reproduced from *Sellers et al.,1996*)

4.5.1 Above the transition layer ($z_t \leq z \leq z_m$)

Conventional log-linear profile is assumed to be valid, and shear stress is assumed to be constant.

$$\tau = \rho K_m \frac{\partial u}{\partial z} \tag{4.39}$$

$$K_m = K_m^* = \kappa u_*(z - d_0) = \frac{\kappa^2 u(z - d_0)}{\log\left(\frac{z - d_0}{z_0}\right)} \tag{4.40}$$

4.5.2 Within the transition layer ($z_2 \leq z \leq z_t$)

Shear stress is assumed to be constant (**eq.4.39**), but the actual value of the momentum transfer coefficient (K_m) varies linearly with height from a value higher than K_m^* (log-linear extrapolated value of K_m) at z_2 to $K_m = K_m^*$ at z_t. This treatment of K_m is intended to take account of the intense local turbulence generated by roughness element at the top of the canopy (Raupach and Thom, 1981; Garrat, 1978).

$$K_m = K_m^* \left[1 + (G_1 - 1)\left(\frac{z_t - z}{z_t - z_2}\right)\right] = \kappa u_*(z - d_0)\left[1 + (G_1 - 1)\left(\frac{z_t - z}{z_t - z_2}\right)\right] \tag{4.41}$$

The transition height itself is assumed to be a linear function of z_0.

$$z_t = z_2 + G_4 z_0 \tag{4.42}$$

To maintain constant shear stress throughout the same layer, the wind velocity gradient must shift away from the log-linear profile.

τ	=	shear stress	$\mathrm{kgm^{-1}s^{-2}}$
K_m	=	local momentum transfer coefficient	$\mathrm{m^2s^{-1}}$
K_m^*	=	log-linear profile value of K_m	$\mathrm{m^2s^{-1}}$
u_*	=	friction velocity	$\mathrm{ms^{-1}}$
u	=	local wind speed	$\mathrm{ms^{-1}}$
d_0	=	zero plane displacement height	m
z_0	=	roughness length	m

4.5.3 Within the canopy air space (CAS) ($z_1 \leq z \leq z_2$)

Leaf area density (L_d) increases with height from z_1 to z_c, after which it decreases linearly with height to z_2, giving a triangular profile of L_d (see **Figure 4.5**).

$$L_d = a_1 + b_1 z \qquad (z_1 < z < z_c) \tag{4.43}$$

$$L_d = a_2 + b_2 z \qquad (z_c < z < z_2) \tag{4.44}$$

$$\tag{4.45}$$

Given an estimate of total leaf area index (L_T) from satellite data, the constants (a_1, a_2, b_1, b_2) can be obtained from the solution of

$$\int_{z_1}^{z_2} L_d dz = L_T \tag{4.46}$$

$$b_1 = \frac{2V_c L_T}{(z_2 - z_1)(z_c - z_1)} \quad b_2 = \frac{2V_c L_T}{(z_2 - z_1)(z_c - z_2)} \quad a_1 = -b_1\ z_1 \quad a_2 = -b_2\ z_2 \tag{4.47}$$

Shear is absorbed by drag force interaction with with the canopy leaves.

$$\frac{\partial \tau}{\partial z} = \rho \frac{C_l L_d}{P_s} u^2 \tag{4.48}$$

Monteith (1973) reproduces data that show the dependence of the leaf drag coefficient of isolated leaves on leaf inclination and dimension.

$$C_l = 1.328\left(\frac{2}{Re^{1/2}}\right) + 0.45\overline{\sin\theta}^{1.6} \tag{4.49}$$

The shelter factor P_s was first introduced by Thom (1972) and is still not well understood. It accounts for the observation that the drag coefficient of an ensemble of densely clustered leaf elements is less than the sum of their individual drag coefficients, presumably due to mutual sheltering effects. Sellers et al. (1996) proposed a power relation function following the observations of Thom (1972).

$$P_s = 1 + L_d^{0.6} \tag{4.50}$$

K_m is assumed to be a product of local wind (u) and mixing length (l_m).

$$K_m = l_m u \qquad l_m = 2(D_l^2\ L_d)^{1/3} \tag{4.51}$$

Following Thom (1971), local wind speed profile within the canopy is simply expressed by an exponential function.

$$u = u_2 \exp\left[-a_w\left(1 - \frac{z}{z_2}\right)\right] \qquad a_w = \left(\frac{C_l\ L_T\ (z_2 - z_1)}{l_m}\right)^{1/2} \tag{4.52}$$

C_l	=	leaf drag coefficient	—
P_s	=	shelter factor of a canopy leaf	—
$\overline{\sin\theta}$	=	mean leaf inclination = (1-χ_L)/π	—
Re	=	Reynolds number = uD_l/v	—
u	=	typical local wind speed ($\simeq$ 1)	m s^{-1}
D_l	=	leaf dimension = $(l_w + l_l)/2$	m
v	=	kinematic viscosity of air ($\simeq 0.15 \times 10^{-4}$ at 15(degC))	m^{2}s^{-1}
u_1, u_2	=	wind speed at z_1, z_2	m s^{-1}

4.5.4 Below the canopy ($z_s \leq z \leq z_1$)

A log-linear wind profile with constant shear stress links the soil surface to the flow at z_1. The shear stress is a function of a ground roughness (z_s).

$$\tau_1 = \rho\left[\frac{\kappa u_1}{\log(z_1/z_s)}\right]^2 \tag{4.53}$$

Thom (1971) defined the zero plane displacement height (d_0) as equivalent to the mement height of momentum absorption by the surface.

$$d_0 = \frac{\displaystyle\int_{z_1}^{z_2} \frac{L_d C_l}{p_s} u^2 z\ dz}{\displaystyle\int_{z_1}^{z_2} \frac{L_d C_l}{p_s} u^2\ dz + \frac{\tau_1}{\rho}} \tag{4.54}$$

4.5.5 Solution of momentum transfer equation set

z_0 and d_0 are independent of wind speed at reference height (u_m). Firstly, the local wind speed at the canopy top is assumed ($u_2 = 1$). Then, wind profile within canopy, u_1, τ_1, d_0, u_* are specified. Next, z_0 is calculated assuming the log-linear profile above the canopy.

$$z_0 = \exp\left(\log(z_2 - d_0) - \frac{\kappa u_2}{u_*}\right) \tag{4.55}$$

Using z_0, d_0, u_*, and u_m, wind speed at canopy top (u_2) is specified, and τ, u_* are modified from the "temporal" values which are specified from ($u_2 = 1$).

$$u_2 = u_m \frac{\log[(z_2 - d_0)/z_0]}{\log[(z_m - d_0)/z_0]} \tag{4.56}$$

$$\tau = \tau u_2^2 \qquad u_* = u_* u_2 \tag{4.57}$$

Now the profile of wind speed (u) and momuntum transfer coefficient (K_m) can be specified from the ground surface (z_s) to the reference height (z_m). These calculated profiles of u and K_m are then used to derive the aerodynamic resistances.

4.5.6 Aerodynamic resistances

The bulk canopy boundary-layer resistance (under neutral condition) is given by following expression.

$$r_b = \left[\int_{z_1}^{z_2} \frac{L_d u^{1/2}}{P_s C_s} dz \right]^{-1} = \frac{C_1}{u_2^{1/2}} \tag{4.58}$$

The transfer coefficient for heat-mass transfer (C_s) is less than that for momentum (C_l) since C_l incorporates both bluff-body and viscous forces, while C_s describes only viscous transfer. Following Goudriaan (1977), C_s is expressed as

$$C_s = 90 l_w^{1/2} \tag{4.59}$$

The ground to canopy air space (CAS) resistance is defined as in SiB.

$$r_d = \int_{z_s}^{h_a} \frac{1}{K_s} dz = \int_{z_s}^{h_a} \frac{1}{K_m} dz = \frac{C_2}{u_2} \tag{4.60}$$

Heat-water vapor transfer coefficient (K_s) is assumed to be equal to K_m.
Canopy source height (h_a) is assumed to be qeual to the center of action of r_b within the canopy as obtained from the solution of

$$\int_{z_1}^{h_a} L_d u^{1/2} dz = \int_{h_a}^{z_2} L_d u^{1/2} dz \tag{4.61}$$

The resistance between CAS and the reference height (z_m) can be described integration of $K_s (= K_m)$ over the distance from h_a to z_m, which includes within-canopy (h_a to z_2), turbulent transition layer (z_2 to z_t) and log-linear profile (z_t to z_m) segments.

$$r_a = \int_{h_a}^{z_m} \frac{1}{K_s} dz = \int_{h_a}^{Z_2} \frac{1}{K_m} dz + \int_{Z_2}^{Z_t} \frac{1}{K_m} dz + \int_{Z_t}^{Z_m} \frac{1}{K_m} dz = \frac{C_3}{u_m} \tag{4.62}$$

The coefficients C_1, C_2, C_3 and the ratio $u_2 : u_m$ need only be calculated once for a given vegetation condition (type, geometry, LAI) to calcurate r_a, r_b, r_d under neutral conditions.
The above expressions for r_a, r_b, r_d are adjusted to take acount of nonneutrality.

$$\frac{1}{r_b} = \frac{u_2^{1/2}}{C_1} + \frac{L_T}{890} \left(\frac{T_c - T_a}{l_w} \right)^{1/4} \tag{4.63}$$

$$\frac{1}{r_d} = \frac{u_2}{C_1} \left[1 + \frac{9 z_2 (T_g - T_a)}{T_g u_2^2} \right] \tag{4.64}$$

$$r_a = \frac{\Psi_M \Psi_H}{\kappa^2 u_m} \tag{4.65}$$

Ψ_M and Ψ_H are integrated universal function of Monin-Obukov similarity (see **Section 2.4**).

4.6 Surface resistances

The surface resistances r_c and r_{surf} are the additional resistances imposed on the transfer of water vapor from leaves' stomata and soil pores.
For bare soil evaporation, r_{surf} is related to the requirement for moisture to diffuse to the soil surface before it can evaporate. r_{surf} governs moisture flux from the top soil layer to the overlying air and was defined following the empirical expression of Shu Fen Sun (1982)

$$r_{surf} = 30 + 3.5W_1^{-2.3} \tag{4.66}$$

When $e_*(T_g) < e_a$, which is the condition of the dew formation (negative evaporation), r_{surf} is set to zero.
For vegetated surfaces, the additional resistance represents the control that 'stomata' exert over transpiration. Stomata are microscopic pores on the leaves of plants that open and close in response to environmental conditions such as PAR, leaf temperature, and soil moisture. Broadly speaking, they seem to maximize rates of plant photosynthesis, while minimizing the risk of excessive transpiration rates which would cause the soil to dry out.
The bulk canopy resistance (r_c) may be thought of as equivalent to all the stomatal resistances of the individual leaves in the canopy "acting in parallel". Accordingly, it is calculated as the total effect of the stomatal resistance of all the leaves in the canopy integrated over all leaf azimuths (ξ), leaf inclinations (θ), and from the top to the bottom of the canopy, that is, over the total leaf area index (L_T). This calculation allows for the effects of differential illumination of individual leaves due to their particular angle to the incoming PAR flux and their position in the canopy. The effects of leaf temperature (T_c), leaf water potential (ψ_l) and vapor pressure deficit (δe) are assumed to act uniformly throughout the canopy and are applied as multiplicative factors to the light-integrated portion of the canopy resistance. r_c may therefore be written as follows.

$$\frac{1}{r_c} = V_c\ N_c\ f(T)\ f(\delta e)\ f(\psi_l) \int_0^{L_T} \int_0^{\pi/2} \int_0^{2\pi} \frac{O(\xi,\theta)}{r_s(F_\pi,\xi,\theta)} \sin\theta\ d\xi\ d\theta\ dL \tag{4.67}$$

Note that r_s is the light-dependent stomatal resistance of an individual leaf, and is given by following expression.

$$r_s = \frac{a_2}{b_2 + \mathbf{F}_\pi \cdot \mathbf{n}} + c_2 \tag{4.68}$$

$f(T_c)$	=	stomatal resistance adjustment factor for the effects of leaf temperature (T_c)
$f(\delta e)$	=	stomatal resistance adjustment factor for the effects of vapor pressure deficit (δe)
$f(\psi_l)$	=	stomatal resistance adjustment factor for the effects of leaf water potential (ψ_l)
$\mathbf{F}_\pi$	=	photosynthetically active radiation (PAR) flux
$\mathbf{n}$	=	vector of leaf normal

The dependence of r_c on different leaf angle distributions is discussed in Sellers (1985). Some analytical solutions to the integral part of **eq.(4.67)** have been obtained for a number of leaf angle distribution functions. However, it is convenient to use the average leaf projection as a function of $\mu, \overline{G(\mu)}$ to replace the leaf angle distribution function $O(\xi,\theta)$. Use of an average leaf projection for given PAR flux direction greatly simplifies the solution of **eq.(4.67)**, as the angular integrations may be dropped.
The use of Ross-Goudriaan function (**eq.(4.28)**) in **eq.(4.67)**, where it replaces the $O(\xi,\theta)\sin\theta$ term, reduces to following formula.

$$\frac{1}{r_c} = V_c\ N_c\ f(T)\ f(\delta e)\ f(\psi_l) \int_0^{L_T} \frac{\overline{G(\mu)}}{r_s}\ dL \tag{4.69}$$

In SiB, the bulked form of **eq.(4.69)** is used in preference to the fully integrated form of **eq.(4.67)**. This necessitates the specification of a single direction for the incoming PAR flux which is made up of both diffuse ($F_{v,d(0)}$) and direct beam ($F_{v,b(0)}$) components. A mean angle of PAR incidence is estimated by considering the "flux-weighted" angles of the direct and diffuse contributions to the total PAR flux.
The value of r_c estimated from the integral parts of **eq.(4.69)** relates only to the PAR dependence of stomatal control, and so represents the minimum attainable value of r_c. The factors outside the integral represent the effects of nonoptimal conditions. The formula was taken from Jarvis (1976) and reproduced in Sellers et al.(1986) and Sellers and Dorman (1987).

$$f(T_c) = \frac{(T_c - T_l)(T_h - T_c)^{h_4}}{(T_o - T_l)(T_h - T_o)^{h_4}} \qquad h_4 = \frac{T_h - T_o}{T_o - T_l} \tag{4.70}$$

$$f(\delta e) = 1 - h_5 \delta e = 1 - h_5[e_*(T_a) - e_a] \tag{4.71}$$

$$f(\psi_l) = \frac{\psi_l - \psi_{c2}}{\psi_{c1} - \psi_{c2}} \tag{4.72}$$

Of particular importance is the factor $f(\psi_l)$ which accounts for the effects of soil moisture stress and excessive evaporation demand. ψ_l is calculated by using catenary model of the water transfer pathway from root zone to leaf (van der Honert, 1948).

$$\psi_l = \psi_r - h_a - \frac{E_{dc}}{\rho_w}(r_{plant} + r_{soil}) \tag{4.73}$$

The soil moisture potential in the root zone ψ_r is obtained by summing the soil moisture potentials weighted by the depth of each soil layer.

$$\psi_r = \frac{1}{D_r}\sum_{0}^{D_r} \psi_i D_i = \frac{\psi_1 D_1 + \psi_2 D_2}{D_r} \tag{4.74}$$

r_{plant} is given as a time-invariant parameter (**Table 4.2**) and r_{soil} is given as a function of ψ_r.
From **eq.(4.73)**, the abstraction of soil moisture by transpiration from the ith soil layer ($E_{dc,i}$) is given by

$$E_{dc,i} = \frac{D_i}{D_r}\left(\frac{\psi_i - \psi_l - h_a}{r_{plant} + r_{soil}}\right)\rho_w \tag{4.75}$$

4.7 Sensible and latent heat fluxes

The fluxes of sensible and latent heat from each surface are described by an Ohm's law analogue form in which the fluxes are propotional to potential differences and inversely propotional to a (series of) resistance.

$$\text{flux} = \frac{\text{potential difference}}{\text{resistance}} \tag{4.76}$$

For the fluxes of sensible heat and latent heat, the potential differences are represented by temperatures and vapor pressures, respectively. The resistances are equivalent to the integrals of inverse conductances over a path between the specified potential difference endpoints. **Figure 4.7(a)** shows how sensible heat fluxes from the canopy (H_c) and the ground (H_g) must traverse the aerodynamic resistances r_b or r_d and r_a. Canopy water vapor flux must traverse an additional resistance (r_c). In addition, since it is assumed that water vapor exchange occurs from only one side of the leaf, the boundary-layer resistance is doubled for water vapor ($2r_b$). Evaporation from

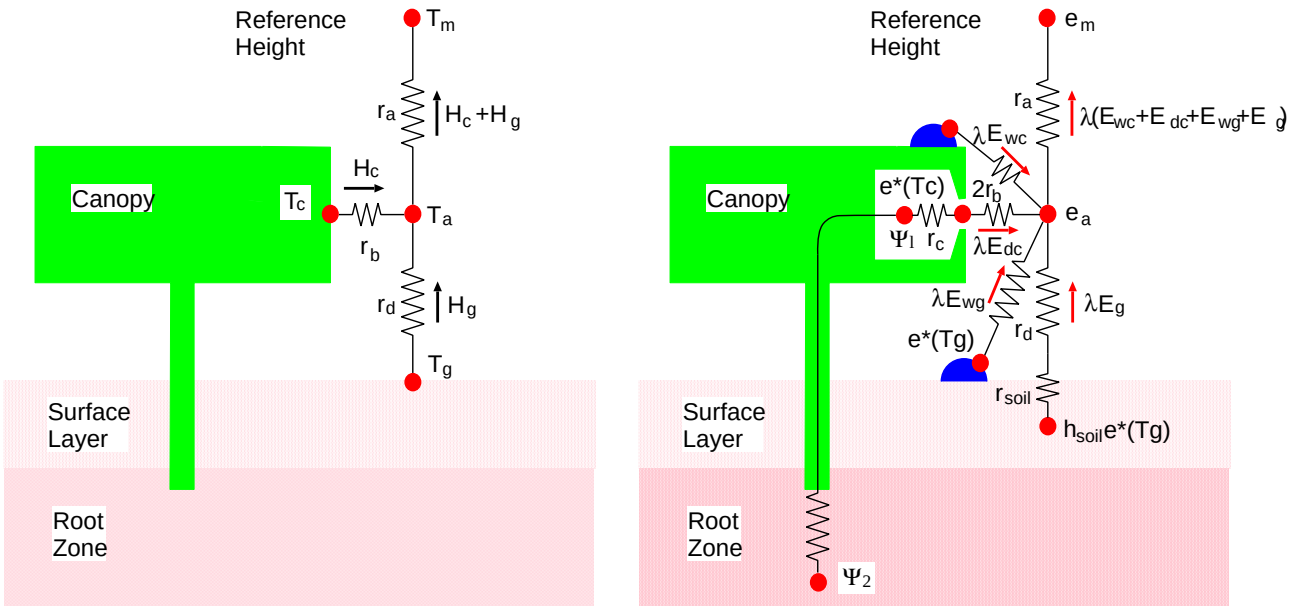

(a) Sensible heat flux (b) Latent heat flux

Figure 4.7: Transfer pathways as conceptualized in the green area model. (Reproduced from *Sellers et al.,1996***)**

within the top soil layer E_g must cross the soil surface resistance (r_{surf}). Fluxes, potential differences, and resistances are summarized in **Table 4.4**. The transfer pathways for sensible and latent heat fluxes are shown schematically in **Figure 4.7**.

Table 4.4: Fluxes, potential differences and resistances associated with green area model

Flux	potential difference	Resistance
H_c	$(T_c - T_a)\rho c_p$	r_b
H_g	$(T_g - T_a)\rho c_p$	r_d
$H_c + H_g$	$(T_a - T_m)\rho c_p$	r_a
λE_{dc}	$(e_*(T_c) - e_a)\rho c_p/\gamma$	$\frac{r_c + 2r_b}{1 - W_c}$
λE_{wc}	$(e_*(T_c) - e_a)\rho c_p/\gamma$	$2r_b/W_c$
λE_s	$(h_{soil}e_*(T_g) - e_a)\rho c_p/\gamma$	$\frac{r_{surf} + r_d}{1 - W_g}$
λE_{wg}	$(e_*(T_g) - e_a)\rho c_p/\gamma$	r_d/W_g
$\lambda(E_c + E_g)$	$(e_a - e_m)\rho c_p/\gamma$	r_a

If we assume no storage of heat at any of the junctions of the resistance network shown in **Figure 4.7(a)**, we can write the area-averaged sensible heat fluxes as follows.

$$H_c = \frac{T_c - T_a}{r_b}\rho C_p = A(T_c - T_a), \qquad A = \rho C_p / r_b \tag{4.77}$$

$$H_g = \frac{T_g - T_a}{r_d}\rho C_p = B(T_g - T_a), \qquad B = \rho C_p / r_d \tag{4.78}$$

$$H_c + H_g = \frac{T_a - T_m}{r_a}\rho C_p = C(T_a - T_m), \qquad C = \rho C_p / r_a \tag{4.79}$$

Air temperature within canopy air space (CAS) (T_a) can be eliminated from **eq.(4.77)** to **(4.79)**.

$$T_a = \frac{A \cdot T_c + B \cdot T_g + C \cdot T_m}{A + B + C} \tag{4.80}$$

Water vapor fluxes from the canopy (E_c) and the ground (E_g) have two components respectively.

E_c	:	E_{wc}	:	evaporation of water from wetted fraction of the canopy (interception loss)
		E_{dc}	:	transpiration of soil water from the dry fraction of the canopy
E_g	:	E_{wg}	:	evaporation of water from wetted fraction of the ground
		E_s	:	direct evaporation of water from the surface soil layer

If we assume no storage of water vapor at any of the junctions of the resistance network shown in **Figure 4.7(b)**, we can write the area-averaged latent heat fluxes as follows.

$$\lambda E_c = \lambda E_{wc} + \lambda E_{dc} = D(e_*(T_c) - e_a), \quad D = \frac{\rho C_p}{\gamma}\left[\frac{W_c}{2r_b} + \frac{1 - W_c}{r_c + 2r_b}\right] \tag{4.81}$$

$$\lambda E_g = \lambda E_{wg} + \lambda E_s = E(e_*(T_g) - e_a), \quad E = \frac{\rho C_p}{\gamma}\left[\frac{W_g}{r_d} + \frac{f_h e_*(T_g) - e_a}{(r_{surf} + r_d)(e_*(T_g) - e_a)}\right] \tag{4.82}$$

$$\lambda E_c + \lambda E_g = F(e_a - e_m), \qquad F = \frac{\rho C_p}{\gamma r_a} \tag{4.83}$$

Water vapor pressure within CAS (e_a) can be eliminated from **eq.(4.81)** to **(4.83)**.

$$e_a = \frac{D \cdot e_*(T_c) + E \cdot e_*(T_g) + F \cdot e_m}{D + E + F} \tag{4.84}$$

4.8 Numerical solution of prognostic equations

In the numerical solution of the prognostic equations for temperatures (T_c, T_g), we make use of the fact that the storage terms, involving $C_i (i = c, g)$, are small relative to the energy fluxes $Rn_i, \lambda E_i, and H_i (i = c, g)$. These values make **eq. (4.2), (4.3)** fast response equations so that changes in T_c, T_g, even over a time step as short as an hour, can have a significant feedback on the magnitude of the energy fluxes. The energy fluxes are explicit functions of atmospheric boundary conditions, prognostic variables, aerodynamic and surface resistances. Prognostic equations are solved by an implicit backward method using partial derivatives of each term.
First, considering the energy fluxes in prognostic equations are functions of temperature, partial derivatives are calculated in subroutine **partial**. Then, prognostic equations are expressed in explicit backward-differencing form and a set of linear simultaneous equations regarding the changes in temperatures over a time step (Δt) are obtained.
Not only energy fluxes but also heat exchange terms have dependency on temperatures. Now prognostic equations can be written in discrete-time form.

$$\begin{aligned} C_c \frac{\Delta T_c}{\Delta t} &= Rn_c - H_c - \lambda E_c \\ &\quad + \left(\frac{\partial Rn_c}{\partial T_c} - \frac{\partial H_c}{\partial T_c} - \frac{\partial \lambda E_c}{\partial T_c}\right)\Delta T_c + \left(\frac{\partial Rn_c}{\partial T_g} - \frac{\partial H_c}{\partial T_g} - \frac{\partial \lambda E_c}{\partial T_g}\right)\Delta T_g \\ C_g \frac{\Delta T_g}{\Delta t} &= Rn_g - H_g - \lambda E_g - \omega C_g (T_g - T_d) + \left(\frac{\partial Rn_g}{\partial T_c} - \frac{\partial H_g}{\partial T_c} - \frac{\partial \lambda E_g}{\partial T_c}\right)\Delta T_c \end{aligned} \tag{4.85}$$

$$+\left(\frac{\partial Rn_g}{\partial T_g}-\frac{\partial H_g}{\partial T_g}-\frac{\partial \lambda E_g}{\partial T_g}-\omega C_g\right)\Delta T_g+\omega C_g\Delta T_d \tag{4.86}$$

$$\begin{aligned} C_d\frac{\Delta T_d}{\Delta t} &= Rn_g-H_g-\lambda E_g \\ &+\left(\frac{\partial Rn_g}{\partial T_c}-\frac{\partial H_g}{\partial T_c}-\frac{\partial \lambda E_g}{\partial T_c}\right)\Delta T_c+\left(\frac{\partial Rn_g}{\partial T_g}-\frac{\partial H_g}{\partial T_g}-\frac{\partial \lambda E_g}{\partial T_g}\right)\Delta T_g \end{aligned} \tag{4.87}$$

If it is written in matrix form,

$$KX=Y \qquad \longrightarrow \qquad X=K^{-1}Y$$

$$K=\begin{bmatrix} K_{1,1} & K_{1,2} & K_{1,3} \\ K_{2,1} & K_{2,2} & K_{2,3} \\ K_{3,1} & K_{3,2} & K_{3,3} \end{bmatrix} \qquad X=\begin{bmatrix} \Delta T_c \\ \Delta T_g \\ \Delta T_d \end{bmatrix}$$

where

$$\begin{array}{lll} K_{1,1}=\dfrac{C_c}{\Delta t}-\dfrac{\partial Rn_c}{\partial T_c}+\dfrac{\partial H_c}{\partial T_c}+\dfrac{\partial \lambda E_c}{\partial T_c} & K_{1,2}=-\dfrac{\partial Rn_c}{\partial T_g}+\dfrac{\partial H_c}{\partial T_g}+\dfrac{\partial \lambda E_c}{\partial T_g} & K_{1,3}=0 \\ K_{2,1}=-\dfrac{\partial Rn_g}{\partial T_c}+\dfrac{\partial H_g}{\partial T_c}+\dfrac{\partial \lambda E_g}{\partial T_c} & K_{2,2}=\dfrac{C_g}{\Delta t}-\dfrac{\partial Rn_g}{\partial T_g}+\dfrac{\partial H_g}{\partial T_g}+\dfrac{\partial \lambda E_g}{\partial T_g}+\omega C_g & K_{2,3}=-\omega C_g \\ K_{3,1}=-\dfrac{\partial Rn_g}{\partial T_c}+\dfrac{\partial H_g}{\partial T_c}+\dfrac{\partial \lambda E_g}{\partial T_c} & K_{3,2}=-\dfrac{\partial Rn_g}{\partial T_g}+\dfrac{\partial H_g}{\partial T_g}+\dfrac{\partial \lambda E_g}{\partial T_g} & K_{3,3}=\dfrac{C_d}{\Delta t} \end{array}$$

$$Y=\begin{bmatrix} Rn_c-H_c-\lambda E_c \\ Rn_g-H_g-\lambda E_g-\omega C_g(T_g-T_d) \\ Rn_g-H_g-\lambda E_g \end{bmatrix}$$

Above equations can be solved in terms of temperature changes $(\Delta T_c, \Delta T_g, \Delta T_d)$. Each temperatures are updated to the value at time $t_0+\Delta t$ by adding temperature changes to the initial value at time t_0. Furthermore, energy fluxes are modified to show the values averaged over a time step (between time t_0 and time $t_0+\Delta t$).

$$Rn'_c = Rn_c+\frac{1}{2}\left(\frac{\partial Rn_c}{\partial T_c}\Delta T_c+\frac{\partial Rn_c}{\partial T_g}\Delta T_g\right) \tag{4.88}$$

$$Rn'_g = Rn_g+\frac{1}{2}\left(\frac{\partial Rn_g}{\partial T_c}\Delta T_c+\frac{\partial Rn_g}{\partial T_g}\Delta T_g\right) \tag{4.89}$$

$$H'_c = H_c+\frac{1}{2}\left(\frac{\partial H_c}{\partial T_c}\Delta T_c+\frac{\partial H_c}{\partial T_g}\Delta T_g\right) \tag{4.90}$$

$$H'_g = H_g+\frac{1}{2}\left(\frac{\partial H_g}{\partial T_c}\Delta T_c+\frac{\partial H_g}{\partial T_g}\Delta T_g\right) \tag{4.91}$$

$$\lambda E'_c = \lambda E_c+\frac{1}{2}\left(\frac{\partial \lambda E_c}{\partial T_c}\Delta T_c+\frac{\partial \lambda E_c}{\partial T_g}\Delta T_g\right) \tag{4.92}$$

$$\lambda E'_g = \lambda E_g+\frac{1}{2}\left(\frac{\partial \lambda E_g}{\partial T_c}\Delta T_c+\frac{\partial \lambda E_g}{\partial T_g}\Delta T_g\right) \tag{4.93}$$

Appendix A

List of simbols and their definitions

Table A.1: List of physical constants

symbol	definition	unit
λ	latent heat of vaporization	J kg^{-1}
c_w	specific heat of water (= 4.18×10^6)	J $m^{-3}K^{-1}$
k_w	thermal conductivity (= 0.6)	W $m^{-1}K^{-1}$
ε_w	emissivity of water (= 0.97)	
σ	Stephan-Boltsman constant (= 5.6698×10^{-8})	$Wm^{-2}K^{-4}$
ρ	density of air (= 1.2)	kg m^{-3}
ρ_w	density of water (=1000)	kg m^{-3}
C_p	specific heat of air (= 1010)	J $kg^{-1}K^{-1}$
γ	psychrometric constant (= 0.662)	mb K^{-1}
ω	angular frequency of diurnal cycle ($2\pi/86400$)	s^{-1}
κ	von Karman's constant (= 0.4)	
g	gravity accerelation (= 9.8)	m s^{-2}